

Group SLOPE Penalized CP Low-Rank Tensor Regression

Yang Chen

School of Mathematics and Statistics, Beijing Jiaotong University, Beijing, China
and

Ziyan Luo*

School of Mathematics and Statistics, Beijing Jiaotong University, Beijing, China

Abstract

This article aims to seek a selection and estimation procedure for a class of tensor regression problems with multivariate covariates and matrix responses, which can provide theoretical guarantees for model selection in finite samples. Considering the frontal slice sparsity and low-rankness inherited in the coefficient tensor, we formulate the regression procedure as a group SLOPE penalized low-rank tensor optimization problem based on CANDECOMP/PARAFAC (CP) decomposition, namely TgSLOPE. This procedure provably controls the newly introduced tensor group false discovery rate (TgFDR), provided that the predictor matrix is column-orthogonal. Moreover, we establish the asymptotically minimax convergence with respect to the ℓ_2 -loss of TgSLOPE estimator at the frontal slice level. For efficient problem resolution, we equivalently transform the TgSLOPE problem into a difference-of-convex (DC) program with the level-coercive objective function. This allows us to solve the reformulation problem of TgSLOPE by an efficient proximal DC algorithm (DCA) with global convergence. Numerical studies conducted on synthetic data and a real human brain connection data illustrate the efficacy of the proposed TgSLOPE estimation procedure.

Keywords: Difference-of-convex, False discovery rate, Group sparsity, Low-rankness, Tensor regression

*Corresponding author. E-mail: zyluo@bjtu.edu.cn.

1 Introduction

Tensor regression modeling, in which the regression coefficients take the form of a multi-way array or tensor, is an important and prevalent technique for coefficient estimation and/or feature selection in the high-dimensional statistical learning theory, with wide applications in many modern data science problems such as neuroimaging analysis, see, e.g., Ahmed et al. (2020), Han et al. (2022), Raskutti et al. (2019), Sun & Li (2017), Zhou et al. (2013). In this article, we focus on the tensor regression with multivariate covariates and matrix responses. Given n independent and identically distributed (i.i.d.) observations $\{(\mathbf{x}_i, \mathbf{Y}_i)\}_{i=1}^n$ with $\mathbf{x}_i \in \mathbb{R}^p$ the vector of predictors and $\mathbf{Y}_i \in \mathbb{R}^{p_1 \times p_2}$ the matrix of responses, the regression model can be expressed as follows

$$\mathbf{Y}_i = \mathcal{B}^* \times_3 \mathbf{x}_i + \mathbf{E}_i, i \in [n] := \{1, 2, \dots, n\}, \quad (1)$$

where $\mathcal{B}^* \in \mathbb{R}^{p_1 \times p_2 \times p}$ is the unknown coefficient tensor with some inheritance structures like sparsity and/or low-rankness, $\mathbf{E}_i, i = 1, \dots, n$, are i.i.d. noise matrices whose entries are i.i.d. drawn from the Gaussian distribution $N(0, \sigma^2)$. Our goal is to seek a feature selection and tensor estimation procedure for model (1). A straightforward idea to estimate \mathcal{B}^* is via optimization problem

$$\hat{\mathcal{B}} = \arg \min_{\mathcal{B} \in \Omega} f(\mathcal{B}; \mathcal{D}),$$

where Ω is any constraint set of sparse and/or low-rank tensors, $f(\mathcal{B}; \mathcal{D})$ can be taken as the least squares loss or any more general loss function with $\mathcal{D} = \{(\mathbf{x}_i, \mathbf{Y}_i)\}_{i=1}^n$ the random sample set.

1.1 Related Work

One simple approach to estimate the sparse and/or low-rank coefficient tensor is to use matricization techniques such that the model (1) is degenerated into a linear matrix regression model, in which the estimated tensor \mathcal{B}^* and the response matrix \mathbf{Y}_i are unfolded into a $p \times p_1 p_2$ matrix and a $p_1 p_2$ dimensional vector, respectively. Therefore, the relevant work on sparse and low-rank matrix regression methods can be applied to deal with the tensor regression problems, see, e.g., group selection by sparsity penalized methods (Chen et al. 2021, Obozinski et al. 2011, Raskutti et al. 2019) and low-rank matrix estimation by reduced-rank regression methods (Bura et al. 2018, Fan et al. 2019, Wei et al. 2021). However, the use of matricization techniques will not only break the sparse and low-rank tensor structures, making resulting estimators difficult to interpret, but also lead to a dramatic increase in dimensionality, which is prone to over-fitting phenomenon.

Keeping the tensor format for the regression model, the existing work can be divided into two categories from the perspective of different characterizations for the sparsity and low-rankness of coefficient tensors. One is based on the tensor decomposition, including CP decomposition (Hao et al. 2020, Sun & Li 2017, Zhou et al. 2013) and Tucker decomposition (Han et al. 2022, Hu et al. 2022, Li et al. 2018, Zhang et al. 2020). The other is the method without tensor decomposition, such as imposing sparsity on elements, fiber vectors, and slice matrices (Raskutti et al. 2019), assuming low-rankness of slice matrices (Chen et al. 2019, Kong et al. 2020, Raskutti et al. 2019), and considering Tucker low-rankness of the coefficient tensor (Chen et al. 2019).

Focusing on the matrix response tensor regression model (1), limited work has been done on statistical property analysis and algorithm design. Sun & Li (2017) have considered an element-wise sparse tensor regression model based on the CP decomposition, and established a non-asymptotic estimation error bound for the estimator obtained from the proposed alternating updating algorithm, which compounds the truncation-based sparse tensor decomposition procedure. Considering

the frontal slice sparsity and low-rankness, Kong et al. (2020) have proposed a two-step screening and estimation procedure and shown that it enjoys estimation consistency and rank consistency. Hu et al. (2022) have developed a generalized Tucker decomposition model with features on multiple modes, and investigated the statistical convergence for the proposed supervised tensor decomposition algorithm with side information. Nevertheless, these methods may not work well for finite samples, since their feature selection results are usually achieved in infinite samples, or unfortunately some of these are not capable of feature selection.

To seek a mechanism that enables to make inference about the validity of the selected model in finite samples, Bogdan et al. (2015) have introduced a new convex penalized method for the classical linear regression inspired by the Benjamini-Hochberg procedure (Benjamini & Hochberg 1995), namely Sorted L-One Penalized Estimation (SLOPE). They have shown that SLOPE controls the false discovery rate (FDR) under certain conditions. Following Bogdan et al. (2015), a recent line of research (Bellec et al. 2018, Brzyski et al. 2019, Luo et al. 2019, Su & Candès 2016, Wei et al. 2021) has studied the SLOPE based methods, including statistical property analysis, algorithm design, etc. One of these work (Brzyski et al. 2019) has extended SLOPE to group SLOPE (gSLOPE) to deal with the situation when one aims to select whole groups of regressors instead of single one. This motivates us to investigate the use of gSLOPE penalty for feature selection and estimation in the tensor regression framework with finite samples.

1.2 Our Contributions

We consider the matrix response tensor regression model (1) and embed the frontal slice sparse and low-rank structures for the estimated tensor \mathcal{B}^* . Unlike the sparse and low-rank settings directly on the frontal slices (Kong et al. 2020), we characterize the inherited structures based on the CP decomposition (which is a form of higher-order principal components analysis, HOPCA). Specifically, we assume that the tensor \mathcal{B}^* enjoys a rank- K CP decomposition in which the produced mode-3 factor matrix admits the row sparsity. We know that the rank- K CP decomposition can reduce the model from ultrahigh dimensionality $p_1 p_2 p$ to $(p_1 + p_2 + p)K$, thereby reducing the computational complexity of the regression procedure. In addition, from the perspective of PCA, the encouraging sparsity of factor matrices has been shown not only to yield asymptotically consistent estimators in high-dimensional settings (Johnstone & Lu 2009), but also to simplify visualization and interpretation of data analysis results (Allen 2012).

To investigate the selection and estimation properties, we develop a sparse and low-rank tensor regression procedure by formulating it as a gSLOPE penalized CP low-rank tensor optimization problem, namely TgSLOPE. Then, to measure its feature selection performance in finite samples, we define the notion of the tensor group FDR (TgFDR). Under the column-orthogonality assumption on the predictor matrix, TgSLOPE is shown to control TgFDR at any given level $0 < q < 1$ with appropriate choice of the regularization parameters. Moreover, the estimator produced by TgSLOPE provably achieves the asymptotically minimax convergence with respect to the ℓ_2 -loss defined based on tensor frontal slices. Overall, our proposed TgFDR controlling estimate achieves the minimax optimal rate.

To well resolve our proposed TgSLOPE model with Stiefel manifold constraints, we constructively reformulate this manifold optimization problem as a difference-of-convex (DC) program whose objective function is shown to be level-coercive. This allows us to adopt some globally convergent DC-type algorithm in which the decision variables are updated by the proximal operator of the gSLOPE penalty. Simulations on synthetic data verify the TgFDR control, and test the effects

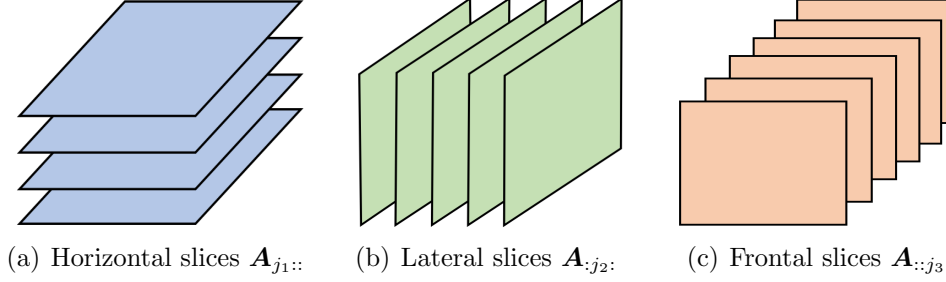


Figure 1: Slices of a order-3 tensor.

of sparsity, model size and CP rank on TgSLOPE performances respectively. In addition, numerical results on both synthetic data and a real human brain connection data confirm the superiority of our proposed TgSLOPE procedure by comparing it with several state-of-the-art approaches.

1.3 Preliminaries and Structure

Throughout the article, we denote scalars, vectors, matrices and tensors by lowercase letters (e.g., a, b), boldface lowercase letters (e.g., \mathbf{a}, \mathbf{b}), boldface uppercase letters (e.g., \mathbf{A}, \mathbf{B}), and calligraphic letters (e.g., \mathcal{A}, \mathcal{B}), respectively. In addition, zero scalars, vectors, matrices and tensors are respectively denoted by $0, \mathbf{0}, \mathbf{O}$ and \mathcal{O} . For a vector $\mathbf{a} \in \mathbb{R}^n$, we denote $\mathbf{a}_{[1:s]} = (a_1, \dots, a_s)^\top$ with $s \leq n$. For a matrix $\mathbf{A} \in \mathbb{R}^{m \times n}$, the i th row is denoted by $\mathbf{a}_{i\cdot}$, and the j th column is denoted by $\mathbf{a}_{\cdot j}$. We also denote $\mathbf{A}_{[i,1:s]} = (\mathbf{a}_{i\cdot 1}, \dots, \mathbf{a}_{i\cdot s})$ with $s \leq n$. Figure 1 shows the horizontal, lateral, and frontal slices of the tensor $\mathcal{A} \in \mathbb{R}^{p_1 \times p_2 \times p_3}$, denoted by $\mathbf{A}_{j_1::} \in \mathbb{R}^{p_2 \times p_3}$, $\mathbf{A}_{:j_2::} \in \mathbb{R}^{p_1 \times p_3}$, and $\mathbf{A}_{::j_3} \in \mathbb{R}^{p_1 \times p_2}$, respectively. For convenience, we simply denote the i th row of \mathbf{A} as \mathbf{a}_i and the j_3 th frontal slice of \mathcal{A} as \mathbf{A}_{j_3} .

Given vectors $\mathbf{a} \in \mathbb{R}^m$ and $\mathbf{b} \in \mathbb{R}^n$, denote the outer product $\mathbf{a} \circ \mathbf{b} = \mathbf{a}\mathbf{b}^\top \in \mathbb{R}^{m \times n}$ and Kronecker product $\mathbf{a} \otimes \mathbf{b} = (a_1\mathbf{b}^\top, \dots, a_m\mathbf{b}^\top)^\top \in \mathbb{R}^{mn}$. For matrices $\mathbf{A} \in \mathbb{R}^{m \times q}$ and $\mathbf{B} \in \mathbb{R}^{n \times q}$, the Khatri-Rao product is defined as $\mathbf{A} \odot \mathbf{B} = (\mathbf{a}_{\cdot 1} \otimes \mathbf{b}_{\cdot 1}, \dots, \mathbf{a}_{\cdot q} \otimes \mathbf{b}_{\cdot q}) \in \mathbb{R}^{mn \times q}$; if $m = n$, the Hadamard product is defined as $\mathbf{A} * \mathbf{B} = [a_{ij}b_{ij}] \in \mathbb{R}^{m \times q}$, and the inner product is defined as $\langle \mathbf{A}, \mathbf{B} \rangle = \sum_{i,j} a_{ij}b_{ij}$. For an order-3 tensor $\mathcal{A} \in \mathbb{R}^{p_1 \times p_2 \times p_3}$, the mode-3 product with a matrix $\mathbf{X} \in \mathbb{R}^{n \times p_3}$ is denoted by $\mathcal{A} \times_3 \mathbf{X} \in \mathbb{R}^{p_1 \times p_2 \times n}$ with elements $(\mathcal{A} \times_3 \mathbf{X})_{i,j,l} = \sum_{k=1}^{p_3} \mathcal{A}_{i,j,k} \mathbf{X}_{l,k}$. We also denote the matricization operator as $\mathcal{M}_3(\cdot)$, which unfolds the tensor \mathcal{A} along the third mode into the matrix $\mathcal{M}_3(\mathcal{A}) \in \mathbb{R}^{p_3 \times p_1 p_2}$. Specifically, $(\mathcal{M}_3(\mathcal{A}))_{k,l} = \mathcal{A}_{i,j,k}$ with $l = 1 + (i-1) + (j-1)p_1$. Then the inverse of mode-3 unfolding can be denoted as $\mathcal{M}_3^{-1}(\cdot)$. The tensor \mathcal{A} is called rank-one if it can be written as the outer product of vectors $\mathcal{A} = \mathbf{u} \circ \mathbf{v} \circ \mathbf{w}$. More about tensor operations can be found in Kolda & Bader (2009).

Next we introduce some norms. For a vector $\mathbf{a} \in \mathbb{R}^n$, denote its ℓ_2 -norm as $\|\mathbf{a}\| = \sqrt{\sum_i a_i^2}$ and ℓ_0 -norm as $\|\mathbf{a}\|_0 = \#\{i : |a_i| \neq 0\}$. For a matrix $\mathbf{A} \in \mathbb{R}^{m \times n}$, denote its Frobenius norm as $\|\mathbf{A}\|_F = \sqrt{\sum_{i,j} a_{ij}^2}$ and trace as $\text{tr}(\mathbf{A}) = \sum_{i=j} a_{ij}$. Write singular values of \mathbf{A} as $\sigma_1(\mathbf{A}) \geq \dots \geq \sigma_p(\mathbf{A})$ with $p = \min\{m, n\}$. Then the nuclear norm is $\|\mathbf{A}\|_* = \sum_k \sigma_k(\mathbf{A})$ and the spectral norm is $\|\mathbf{A}\|_2 = \sigma_1(\mathbf{A})$. We also introduce the notation $\|\mathbf{A}\| = (\|\mathbf{a}_1\|, \dots, \|\mathbf{a}_m\|)^\top$ for any matrix $\mathbf{A} \in \mathbb{R}^{m \times n}$ and $\|\mathcal{A}\|_F = (\|\mathbf{A}_1\|_F, \dots, \|\mathbf{A}_{p_3}\|_F)^\top$ for any tensor $\mathcal{A} \in \mathbb{R}^{p_1 \times p_2 \times p_3}$.

Moreover, we say that a random variable X has a chi distribution with n degrees of freedom, written by $X \sim \chi_n$, if it is the square root of a chi-squared random variable, i.e., $X^2 \sim \chi_n^2$.

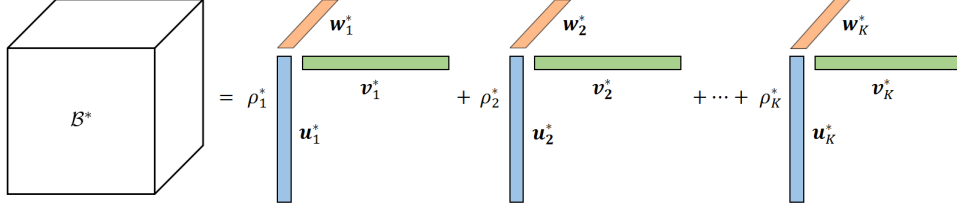


Figure 2: Illustration of the rank- K CP decomposition of the tensor \mathcal{B}^* .

For a proper closed convex function $f : \mathbb{R}^{m \times n} \rightarrow (-\infty, \infty]$, the subdifferential of f at any given $\mathbf{X} \in \text{dom}(f)$, says $\partial f(\mathbf{X})$, is defined by

$$\partial f(\mathbf{X}) = \{\mathbf{G} \in \mathbb{R}^{m \times n} : f(\mathbf{Y}) \geq f(\mathbf{X}) + \langle \mathbf{G}, \mathbf{Y} - \mathbf{X} \rangle \text{ for all } \mathbf{Y} \in \mathbb{R}^{m \times n}\},$$

where each matrix $\mathbf{G} \in \partial f(\mathbf{X})$ is called a subgradient of f at \mathbf{X} . The proximal operator of f is given by

$$\text{Prox}_f(\mathbf{X}) = \arg \min_{\mathbf{Z}} \left\{ f(\mathbf{Z}) + \frac{1}{2} \|\mathbf{Z} - \mathbf{X}\|_F^2 \right\}, \quad \forall \mathbf{X} \in \mathbb{R}^{m \times n}.$$

Given positive scalars a and b , denote $a \sim b$ if $a/b \rightarrow 1$, and $a \asymp b$ if there exist uniform constants $c, C > 0$ such that $ca \leq b \leq Ca$.

The remainder of this article is organized as follows. In Section 2, we introduce a frontal slice sparse and low-rank tensor regression procedure, which optimizes the gSLOPE penalized CP low-rank tensor optimization problem. Section 3 makes statistical theory analysis for TgSLOPE procedure, including the TgFDR control at the prespecified level and the asymptotically minimax convergence with respect to the ℓ_2 -loss. An efficient and globally convergent pDCAe algorithm is proposed in Section 4. Section 5 reports some numerical studies to verify performances of our proposed TgSLOPE approach. Concluding remarks are drawn in Section 6.

2 Model

In this section, we propose a feature selection and tensor estimate method for the tensor regression model (1), which can also be rewritten as

$$\mathcal{Y} = \mathcal{B}^* \times_3 \mathbf{X} + \mathcal{E}, \quad (2)$$

where $\mathcal{Y}, \mathcal{E} \in \mathbb{R}^{p_1 \times p_2 \times n}$, $\mathbf{X} \in \mathbb{R}^{n \times p}$. As discussed above, it is crucial to introduce some sparse and low-rank structures in order to facilitate estimation of the ultrahigh dimensional unknown parameters in finite samples. Thus, for the efficient feature selection, we consider the frontal slice sparsity based on the CP decomposition in the tensor regression framework (2).

Assume that the coefficient tensor \mathcal{B}^* admits a rank- K CP decomposition which models a tensor as a sum of K rank-one tensors (Kolda & Bader 2009). Specifically, $\mathcal{B}^* = \sum_{k=1}^K \rho_k^* \mathbf{u}_k^* \circ \mathbf{v}_k^* \circ \mathbf{w}_k^*$, where the factor vectors $\mathbf{u}_k^* \in \mathbb{R}^{p_1}$, $\mathbf{v}_k^* \in \mathbb{R}^{p_2}$, $\mathbf{w}_k^* \in \mathbb{R}^p$, $k = 1, \dots, K$ are normalized to length one with the weights absorbed into $\boldsymbol{\rho}^* = (\rho_1^*, \rho_2^*, \dots, \rho_K^*)^T$. Figure 2 illustrates the rank- K CP decomposition. Denote the factor matrices composed of the vectors from the rank-one components by $\mathbf{U}^* = (\mathbf{u}_1^*, \mathbf{u}_2^*, \dots, \mathbf{u}_K^*) \in \mathbb{R}^{p_1 \times K}$, $\mathbf{V}^* \in \mathbb{R}^{p_2 \times K}$ and $\mathbf{W}^* \in \mathbb{R}^{p \times K}$ respectively. Following the matricized form of a tensor, we have $\mathcal{M}_3(\mathcal{B}^*) = \mathbf{W}^* \boldsymbol{\Sigma}^* (\mathbf{V}^* \odot \mathbf{U}^*)^T$ with $\boldsymbol{\Sigma}^* = \text{Diag}(\boldsymbol{\rho}^*) \in \mathbb{R}^{K \times K}$ the

positive diagonal matrix. Motivated by the tensor singular value decomposition (SVD) (Poythressa et al. 2021, Zhang & Golub 2001), we further assume that \mathcal{B}^* is orthogonally decomposable, that is, the factor matrices produced by CP decomposition are column-orthogonal. This guarantees the uniqueness of CP decomposition under the restraint of $\rho_1^* \geq \dots \geq \rho_K^* > 0$. Moreover, we consider row sparsity settings on the mode-3 factor matrix \mathbf{W}^* , which can translate to the sparsity of the frontal slices for the tensor \mathcal{B}^* .

To identify significant features and estimate the coefficient tensor \mathcal{B}^* , we develop a penalized sparse and low-rank tensor regression method which optimizes the following gSLOPE penalized CP low-rank tensor optimization problem (TgSLOPE)

$$\begin{aligned} \min_{\mathbf{U}, \mathbf{V}, \mathbf{W}, \Sigma} \quad & \frac{1}{2} \|\mathcal{M}_3(\mathcal{Y}) - \mathbf{X}\mathbf{W}\Sigma(\mathbf{V} \odot \mathbf{U})^\top\|_F^2 + P_\lambda(\llbracket \mathbf{W}\Sigma \rrbracket) \\ \text{s.t.} \quad & \mathbf{U}^\top \mathbf{U} = \mathbf{V}^\top \mathbf{V} = \mathbf{W}^\top \mathbf{W} = \mathbf{I}_K, \Sigma \succ \mathbf{O}, \end{aligned} \quad (3)$$

where $P_\lambda(\mathbf{x}) = \sum_{j=1}^p \lambda_j |x|_{(j)}$ is the SLOPE penalty with the regularization parameter vector $\boldsymbol{\lambda} = (\lambda_1, \dots, \lambda_p)^\top$ satisfying

$$\lambda_1 \geq \lambda_2 \geq \dots \geq \lambda_p \geq 0 \text{ and } \lambda_1 > 0,$$

and $|x|_{(j)}$ the j th largest component of \mathbf{x} in magnitude.

According to the property of the matrix Khatri-Rao product that for any $\mathbf{A} \in \mathbb{R}^{m \times k}$ and $\mathbf{B} \in \mathbb{R}^{n \times k}$, $(\mathbf{A} \odot \mathbf{B})^\top (\mathbf{A} \odot \mathbf{B}) = (\mathbf{A}^\top \mathbf{A}) * (\mathbf{B}^\top \mathbf{B})$, we have the following lemma.

Lemma 1 *For any two column-orthogonal matrices $\mathbf{A} \in \mathbb{R}^{m \times k}$ and $\mathbf{B} \in \mathbb{R}^{n \times k}$, we have $\mathbf{C} = \mathbf{A} \odot \mathbf{B} \in \mathbb{R}^{mn \times k}$ is column-orthogonal, that is, $\mathbf{C}^\top \mathbf{C} = \mathbf{I}_k$.*

Denote $\mathbf{G}^* = \mathbf{W}^* \Sigma^* \in \mathbb{R}^{p \times K}$ and $\mathbf{H}^* = \mathbf{V}^* \odot \mathbf{U}^* \in \mathbb{R}^{p_1 p_2 \times K}$. Without loss of generality, we assume that $K \leq \min\{p, p_1 p_2\}$. It is known from Lemma 1 that $\mathbf{H}^{*\top} \mathbf{H}^* = \mathbf{I}_K$. Thus, the TgSLOPE problem (3) can be simplified as

$$\begin{aligned} \min_{\mathbf{G}, \mathbf{H}} \quad & L(\mathbf{G}, \mathbf{H}) + P_\lambda(\llbracket \mathbf{G} \rrbracket) \\ \text{s.t.} \quad & \mathbf{H}^\top \mathbf{H} = \mathbf{I}_K, \end{aligned} \quad (4)$$

where the loss $L(\mathbf{G}, \mathbf{H}) = \frac{1}{2} \|\mathcal{M}_3(\mathcal{Y}) - \mathbf{X}\mathbf{G}\mathbf{H}^\top\|_F^2$. The estimator $(\hat{\mathbf{G}}, \hat{\mathbf{H}})$ produced by (4) and the tensor estimator $\hat{\mathcal{B}}$ are linked via $\hat{\mathcal{B}} = \mathcal{M}_3^{-1}(\hat{\mathbf{G}}\hat{\mathbf{H}}^\top)$.

3 Statistical Results

This section is devoted to the TgFDR control and the estimate accuracy for our proposed TgSLOPE procedure in finite samples.

3.1 TgFDR Control

FDR is a commonly used error rate that counts the expected proportion of errors among the rejected hypotheses in multiple testing. In this subsection, we develop the classic FDR notion to the setting of tensor regression and show that it can be well controlled by our proposed TgSLOPE.

Definition 1 Consider the tensor regression model (2) and let $(\hat{\mathbf{G}}, \hat{\mathbf{H}})$ be an estimator given by the optimization problem (4). We define the tensor group false discovery rate (TgFDR) for TgSLOPE as

$$\text{TgFDR} = \mathbb{E} \left[\frac{V}{\max\{R, 1\}} \right], \quad (5)$$

where V, R are defined as follows

$$V = \#\{j \in [p] : \mathbf{g}_j^* = \mathbf{0}, \hat{\mathbf{g}}_j \neq \mathbf{0}\}, \quad R = \#\{j \in [p] : \hat{\mathbf{g}}_j \neq \mathbf{0}\} \quad (6)$$

with \mathbf{g}_j^* and $\hat{\mathbf{g}}_j$ the j th rows of \mathbf{G}^* and $\hat{\mathbf{G}}$, respectively.

Theorem 1 Consider the tensor regression model (2) with the predictor matrix \mathbf{X} satisfying $\mathbf{X}^T \mathbf{X} = \mathbf{I}_p$. Define the regularization parameters of the TgSLOPE procedure as

$$\lambda_j = \sigma F_{\chi_K}^{-1}(1 - q \cdot j/p), \quad j \in [p], \quad (7)$$

where $0 < q < 1$, $F_{\chi_K}^{-1}(\alpha)$ is the α th quantile of the χ distribution with K degrees of freedom. Then, for any solution $(\hat{\mathbf{G}}, \hat{\mathbf{H}})$ given by the TgSLOPE problem (4), TgFDR obeys

$$\text{TgFDR} = \mathbb{E} \left[\frac{V}{\max\{R, 1\}} \right] \leq q \cdot \frac{p-s}{p}$$

with s the number of nonzero rows of \mathbf{G}^* .

Proof. Assume that $(\hat{\mathbf{G}}, \hat{\mathbf{H}})$ is an optimal solution of the TgSLOPE problem (4). Let $\hat{\mathbf{H}}^\perp \in \mathbb{R}^{p_1 p_2 \times (p_1 p_2 - K)}$ such that $[\hat{\mathbf{H}}, \hat{\mathbf{H}}^\perp]$ is orthogonal. Then the loss function of problem (4)

$$\begin{aligned} L(\mathbf{G}, \hat{\mathbf{H}}) &= \left\| [\mathcal{M}_3(\mathcal{Y}) - \mathbf{X} \mathbf{G} \hat{\mathbf{H}}^T] [\hat{\mathbf{H}}, \hat{\mathbf{H}}^\perp] \right\|_F^2 \\ &= \left\| \mathcal{M}_3(\mathcal{Y}) \hat{\mathbf{H}} - \mathbf{X} \mathbf{G} \right\|_F^2 + \left\| \mathcal{M}_3(\mathcal{Y}) \hat{\mathbf{H}}^\perp \right\|_F^2. \end{aligned}$$

Together with the column-orthogonality of the predictor matrix \mathbf{X} , we have

$$\hat{\mathbf{G}} = \arg \min_{\mathbf{G} \in \mathbb{R}^{p \times K}} \left\{ \frac{1}{2} \left\| \hat{\mathbf{Y}} - \mathbf{G} \right\|_F^2 + P_\lambda(\|\mathbf{G}\|) \right\}, \quad (8)$$

where $\hat{\mathbf{Y}} = \mathbf{X}^T \mathcal{M}_3(\mathcal{Y}) \hat{\mathbf{H}} \in \mathbb{R}^{p \times K}$. It follows from (2) that

$$\hat{\mathbf{Y}} = \mathbf{G}^* \mathbf{H}^{*T} \hat{\mathbf{H}} + \mathbf{X}^T \mathcal{M}_3(\mathcal{E}) \hat{\mathbf{H}},$$

which implies that $\hat{\mathbf{Y}}$ follows the matrix normal distribution $\mathcal{N}(\mathbf{G}^* \mathbf{H}^{*T} \hat{\mathbf{H}}, \sigma^2 \mathbf{I}_p \otimes \mathbf{I}_K)$. Note that (8) is a convex problem with strongly convex, piecewise linear-quadratic objective function and hence admits a unique optimal solution. Similar to the proximal operator for gSLOPE (Brzyski et al. 2019), the optimization problem (8) can be solved in two steps

$$\begin{cases} \hat{\boldsymbol{\eta}} = \arg \min_{\boldsymbol{\eta}} \left\{ \frac{1}{2} \sum_{j=1}^p (\|\hat{\boldsymbol{\eta}}_j\| - \eta_j)^2 + P_\lambda(\boldsymbol{\eta}) \right\}, \\ \hat{\mathbf{g}}_j = \hat{\boldsymbol{\eta}}_j \frac{\hat{\boldsymbol{\eta}}_j}{\|\hat{\boldsymbol{\eta}}_j\|}, j \in [p]. \end{cases} \quad (9)$$

Define $V_\eta = \#\{j \in [p] : \mathbf{g}_j^* = \mathbf{0}, \hat{\eta}_j \neq 0\}$, $R_\eta = \#\{j \in [p] : \hat{\eta}_j \neq 0\}$. It suffices to show that

$$\mathbb{E} \left[\frac{V_\eta}{\max\{R_\eta, 1\}} \right] \leq q \cdot \frac{p-s}{p}.$$

Without loss of generality, assume that $\mathbf{g}_j^* = \mathbf{0}$ for $0 \leq j \leq p-s$ and $\mathbf{g}_j^* \neq \mathbf{0}$ otherwise. By the definition of TgFDR, we derive that

$$\begin{aligned} \mathbb{E} \left[\frac{V_\eta}{\max\{R_\eta, 1\}} \right] &= \sum_{r=1}^p \frac{1}{r} \mathbb{E} [V_\eta \mathbb{1}_{\{R_\eta=r\}}] \\ &= \sum_{r=1}^p \frac{1}{r} \sum_{j=1}^{p-s} \mathbb{E} [\mathbb{1}_{\{\hat{\eta}_j \neq 0\}} \mathbb{1}_{\{R_\eta=r\}}] \\ &= \sum_{r=1}^p \frac{1}{r} \sum_{j=1}^{p-s} \Pr(\hat{\eta}_j \neq 0, R_\eta = r), \end{aligned} \tag{10}$$

where $\mathbb{1}_{\{\cdot\}} = 1$ if the event occurs, and $\mathbb{1}_{\{\cdot\}} = 0$ otherwise. Next we focus on the events $\{\hat{\eta}_j \neq 0, R_\eta = r\}$, $j = 1, \dots, p-s, r = 1, \dots, p$. Denote $\bar{\mathbf{Y}} = (\hat{\mathbf{y}}_1, \dots, \hat{\mathbf{y}}_{j-1}, \hat{\mathbf{y}}_{j+1}, \dots, \hat{\mathbf{y}}_p)^\top \in \mathbb{R}^{(p-1) \times K}$, $\bar{\boldsymbol{\lambda}} = (\lambda_2, \dots, \lambda_p)^\top \in \mathbb{R}^{p-1}$. Applying the simplified TgSLOPE problem (8) to $\bar{\mathbf{Y}}$ with tuning parameter $\bar{\boldsymbol{\lambda}}$, the optimization problem is given by

$$\bar{\mathbf{G}} = \arg \min_{\mathbf{G} \in \mathbb{R}^{(p-1) \times K}} \left\{ \frac{1}{2} \sum_{j=1}^{p-1} \|\bar{\mathbf{y}}_j - \mathbf{g}_j\|^2 + P_{\bar{\boldsymbol{\lambda}}}(\|\mathbf{G}\|) \right\}.$$

Define $\bar{R}^j = \#\{j \in [p-1] : \bar{\mathbf{g}}_j \neq \mathbf{0}\}$. It follows from Lemmas E.6 and E.7 in Brzyski et al. (2019) that

$$\{[\hat{\mathbf{Y}}] : \hat{\eta}_j \neq 0, R_\eta = r\} \subset \{[\hat{\mathbf{Y}}] : \|\hat{\mathbf{y}}_j\| > \lambda_r, \bar{R}^j = r-1\},$$

where $[\hat{\mathbf{Y}}] = (\|\hat{\mathbf{y}}_1\|, \dots, \|\hat{\mathbf{y}}_p\|)^\top$ with $\|\hat{\mathbf{y}}_j\|^2 \sim \chi_K^2(\|\mathbf{g}_j^* \mathbf{H}^{*T} \hat{\mathbf{H}}\|^2)$, $j = 1, \dots, p$. Then we have

$$\begin{aligned} \Pr(\hat{\eta}_j \neq 0, R_\eta = r) &\leq \Pr(\|\hat{\mathbf{y}}_j\| > \lambda_r, \bar{R}^j = r-1) \\ &= \Pr(\|\hat{\mathbf{y}}_j\|/\sigma > \lambda_r^*) \Pr(\bar{R}^j = r-1) \\ &\leq \frac{q \cdot r}{p} \Pr(\bar{R}^j = r-1), \end{aligned}$$

where $\lambda_r^* = F_{\chi_K}^{-1}(1 - q \cdot r/p)$, the equality is due to the independence between $\|\hat{\mathbf{y}}_j\|$ and \bar{R}^j , the last inequality follows from the definition of the tuning parameters in (7). Therefore, TgFDR in (10) can be bounded by

$$\begin{aligned} \mathbb{E} \left[\frac{V_\eta}{\max\{R_\eta, 1\}} \right] &\leq \sum_{r=1}^p \frac{1}{r} \sum_{j=1}^{p-s} \frac{q \cdot r}{p} \Pr(\bar{R}^j = r-1) \\ &= \sum_{j=1}^{p-s} \frac{q}{p} \sum_{r=1}^p \Pr(\bar{R}^j = r-1) = q \cdot \frac{p-s}{p}. \end{aligned}$$

The proof is completed. \square

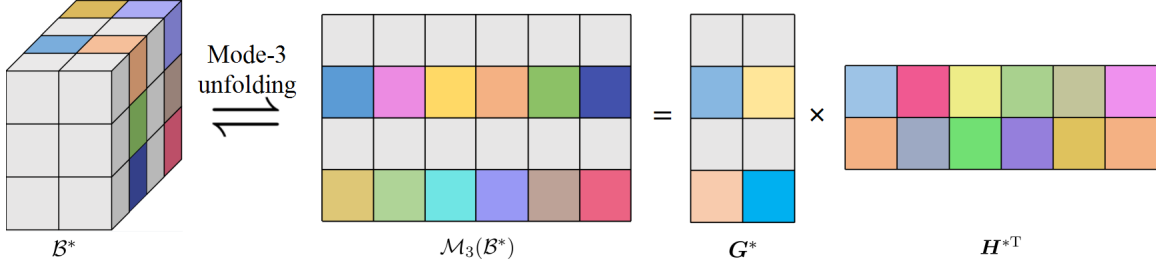


Figure 3: Illustration of the sparsity equivalence relation between factor matrix \mathbf{G}^* and tensor \mathcal{B}^* . Here the elements of matrices and tensors are zero (gray) and nonzero (colour).

Remark 1 *Owing to the uniqueness of the orthogonal CP decomposition claimed by Zhang & Golub (2001), our row sparsity settings on the matrix \mathbf{G}^* can be equivalently interpreted as the sparsity in the frontal slices of the coefficient tensor \mathcal{B}^* . Figure 3 illustrates this equivalence relation. Therefore, the definition of TgFDR in (5) can be redefined based on the following random variables*

$$TV = \#\{j \in [p] : \mathbf{B}_j^* = \mathbf{O}, \hat{\mathbf{B}}_j \neq \mathbf{O}\}, \quad TR = \#\{j \in [p] : \hat{\mathbf{B}}_j \neq \mathbf{O}\}$$

with \mathbf{B}_j^* and $\hat{\mathbf{B}}_j$ the j th frontal slices of \mathcal{B}^* and $\hat{\mathcal{B}}$, respectively. This indicates that the estimator $\hat{\mathcal{B}} = \mathcal{M}_3^{-1}(\hat{\mathbf{G}}\hat{\mathbf{H}}^T)$ given by (4) provably controls TgFDR at any prespecified level $q \in (0, 1)$.

3.2 Estimate Accuracy

This subsection aims to show that TgSLOPE enjoys minimax optimal estimation property under the assumption that the ground truth \mathcal{B}^* is bounded, that is, $\max\{\|\mathbf{B}_j^*\|_F, j \in [p]\} < \infty$. We measure the deviation of an estimator from \mathcal{B}^* at the frontal slice level in the following theorem.

Theorem 2 *Consider the TgSLOPE optimization problem (4) with the predictor matrix \mathbf{X} satisfying $\mathbf{X}^T \mathbf{X} = \mathbf{I}_p$ and the regularization parameter vector $\boldsymbol{\lambda} = (\lambda_1, \dots, \lambda_p)^T$ following the definition in (7). Then, under $p \rightarrow \infty$ and $s/p \rightarrow 0$, the TgSLOPE estimator $\hat{\mathcal{B}}$ obeys that*

$$\sup_{\mathcal{B}^* \in \mathbb{B}_s} \mathbb{E} \|\llbracket \hat{\mathcal{B}} \rrbracket_F - \llbracket \mathcal{B}^* \rrbracket_F\|^2 = (1 + o(1))2\sigma^2 s \log(p/s), \quad (11)$$

where $\mathbb{B}_s = \{\mathcal{B} : \|\llbracket \mathcal{B} \rrbracket_F\|_0 \leq s\}$.

Proof. Let $(\hat{\mathbf{G}}, \hat{\mathbf{H}})$ be an optimal solution of the problem (4). Then $\hat{\mathcal{B}} = \mathcal{M}_3^{-1}(\hat{\mathbf{G}}\hat{\mathbf{H}}^T)$. Under the column-orthogonality assumption on the predictor matrix \mathbf{X} , we know that the statistically equivalent model of (2) is

$$\tilde{\mathbf{Y}} = \mathcal{M}_3(\mathcal{B}^*) + \mathbf{X}^T \mathcal{M}_3(\mathcal{E}), \quad (12)$$

which has the distribution $\mathcal{N}(\mathcal{M}_3(\mathcal{B}^*), \sigma^2 \mathbf{I}_p \otimes \mathbf{I}_K)$. Denote $\tilde{\mathbb{B}}$ as the set of all coefficient tensors for which only the elements in the first column of the mode-3 unfolded matrix are possibly nonzero and the rest are fixed to be zero. Let $\tilde{\mathbb{B}}_s = \mathbb{B}_s \cap \tilde{\mathbb{B}}$. Then, for any $\mathcal{B}^* \in \tilde{\mathbb{B}}_s$, (12) is reduced to a

general Gaussian sequence model with length p and sparsity at most s . As $s/p \rightarrow 0$, the model has minimax risk $(1 + o(1))2\sigma^2 s \log(p/s)$ (Donoho & Johnstone 1994). Thus, we have

$$\sup_{\mathcal{B}^* \in \tilde{\mathbb{B}}_s} \mathbb{E} \|\mathcal{M}(\hat{\mathcal{B}}) - \mathcal{M}(\mathcal{B}^*)\|_F^2 \geq (1 + o(1))2\sigma^2 s \log(p/s),$$

which yields that

$$\sup_{\mathcal{B}^* \in \mathbb{B}_s} \mathbb{E} \|\llbracket \hat{\mathcal{B}} \rrbracket_F - \llbracket \mathcal{B}^* \rrbracket_F\|^2 \geq (1 + o(1))2\sigma^2 s \log(p/s).$$

We next show that the ℓ_2 -loss which measures the deviation of the TgSLOPE estimator from the ground truth \mathcal{B}^* is bounded above by $(1 + o(1))2\sigma^2 s \log(p/s)$. For simplicity, we assume that $\|\mathbf{g}_j^*\| \neq 0$ for $j \leq s$ and $\|\mathbf{g}_j^*\| = 0$ otherwise. Denote $\mu_j = \|\mathbf{g}_j^*\|$ and $\nu_j = \|\mathbf{g}_j^* \mathbf{H}^{*\top} \hat{\mathbf{H}}\|$. Then, it follows from the proof of Theorem 1 that $\hat{\mathbf{G}}$ can be obtained by the two step format (9), in which $\|\hat{\mathbf{y}}_j\|^2 \sim \chi_K^2(\nu_j^2)$, $j = 1, \dots, p$. The ℓ_2 -loss is

$$\begin{aligned} \mathbb{E} \|\llbracket \hat{\mathcal{B}} \rrbracket_F - \llbracket \mathcal{B}^* \rrbracket_F\|^2 &= \mathbb{E} \|\llbracket \hat{\mathbf{G}} \hat{\mathbf{H}}^\top \rrbracket - \llbracket \mathbf{G}^* \mathbf{H}^{*\top} \rrbracket\|^2 = \mathbb{E} \|\llbracket \hat{\mathbf{G}} \rrbracket - \llbracket \mathbf{G}^* \rrbracket\|^2 \\ &= \mathbb{E} \left[\sum_{j=1}^s (\|\hat{\mathbf{g}}_j\| - \|\mathbf{g}_j^*\|)^2 \right] + \mathbb{E} \left[\sum_{j=s+1}^p \|\hat{\mathbf{g}}_j\|^2 \right] \\ &= \underbrace{\mathbb{E} \left[\sum_{j=1}^s (\hat{\eta}_j - \mu_j)^2 \right]}_{E1} + \underbrace{\mathbb{E} \left[\sum_{j=s+1}^p \hat{\eta}_j^2 \right]}_{E2}, \end{aligned}$$

where the first equality is due to $\hat{\mathcal{B}} = \mathcal{M}_3^{-1}(\hat{\mathbf{G}} \hat{\mathbf{H}}^\top)$, and the second equality follows from the column-orthogonality of $\hat{\mathbf{H}}$ and \mathbf{H} . Thus, it suffices to show

$$E1 \leq (1 + o(1))2\sigma^2 s \log(p/s) \quad \text{and} \quad E2 = o(1)2\sigma^2 s \log(p/s).$$

To proceed, define random variables $\psi_j^2 = \psi_{j,1}^2 + \psi_{j,2}^2 + \dots + \psi_{j,K}^2$ and $\phi_j^2 = (\psi_{j,1} + \nu_j)^2 + \psi_{j,2}^2 + \dots + \psi_{j,K}^2$ with i.i.d. $\psi_{j,k} \sim N(0, 1)$, $j \in [p]$, $k \in [K]$. Then $\psi_j^2 \sim \chi_K^2$ and $\phi_j^2 \sim \chi_K^2(\nu_j^2)$ for all $j \in [p]$. Denoting $\boldsymbol{\phi} = (\phi_1, \phi_2, \dots, \phi_p)^\top$, we have

$$\begin{aligned} \mathbb{E} \|\hat{\boldsymbol{\eta}}_{[1:s]} - \boldsymbol{\mu}_{[1:s]}\|^2 &= \mathbb{E} \|\hat{\boldsymbol{\eta}}_{[1:s]} - \boldsymbol{\phi}_{[1:s]} + \boldsymbol{\phi}_{[1:s]} - \boldsymbol{\mu}_{[1:s]}\|^2 \\ &\leq \mathbb{E} \left(\|\hat{\boldsymbol{\eta}}_{[1:s]} - \boldsymbol{\phi}_{[1:s]}\| + \|\boldsymbol{\phi}_{[1:s]} - \boldsymbol{\mu}_{[1:s]}\| \right)^2 \\ &\leq \|\boldsymbol{\lambda}_{[1:s]}\|^2 + \mathbb{E} \|\boldsymbol{\phi}_{[1:s]} - \boldsymbol{\mu}_{[1:s]}\|^2 + 2\|\boldsymbol{\lambda}_{[1:s]}\| \mathbb{E} \|\boldsymbol{\phi}_{[1:s]} - \boldsymbol{\mu}_{[1:s]}\|, \end{aligned} \tag{13}$$

where the last inequality is obtained by $\|\hat{\boldsymbol{\eta}}_{[1:s]} - \boldsymbol{\phi}_{[1:s]}\| \leq \|\boldsymbol{\lambda}_{[1:s]}\|$, owing to Fact 3.3 of Su & Candès (2016) with conditions ϕ_j^2 and $\|\hat{\mathbf{y}}_j\|^2$ are i.i.d. for any $j \leq s$. Moreover, it follows from Inglot (2010) that as $s/p \rightarrow 0$, $F_{\chi_K}^{-1}(1 - q \cdot j/p) \sim \sqrt{2 \log(p/(q \cdot j))}$ for all $j \leq s$, which yields

$$\|\boldsymbol{\lambda}_{[1:s]}\|^2 \sim 2\sigma^2 s \log(p/s). \tag{14}$$

Then, it is easy to see that

$$\begin{aligned}
|\phi_j - \mu_j|^2 &= \left| \sqrt{(\psi_{j,1} + \nu_j)^2 + \psi_{j,2}^2 + \cdots + \psi_{j,K}^2} - \mu_j \right|^2 \\
&\leq \left| \sqrt{\psi_{j,2}^2 + \cdots + \psi_{j,K}^2} + |\psi_{j,1} + \nu_j - \mu_j| \right|^2 \\
&\leq \left(\sqrt{2(\psi_{j,1}^2 + \psi_{j,2}^2 + \cdots + \psi_{j,K}^2)} + |\nu_j - \mu_j| \right)^2 \\
&\leq 4\psi_j^2 + 2(\nu_j - \mu_j)^2.
\end{aligned} \tag{15}$$

Plugging $\mu_j = \|\mathbf{g}_j^*\|$ and $\nu_j = \|\mathbf{g}_j^* \mathbf{H}^{*\top} \hat{\mathbf{H}}\|$ into the part $|\nu_j - \mu_j|$ derives that

$$\begin{aligned}
|\nu_j - \mu_j| &\stackrel{(a)}{\leq} \|\mathbf{g}_j^* \mathbf{H}^{*\top} \hat{\mathbf{H}} - \mathbf{g}_j^*\| = \|(\mathcal{M}_3(\mathcal{B}^*))_j(\hat{\mathbf{H}} - \mathbf{H}^*)\| \\
&\leq \|(\mathcal{M}_3(\mathcal{B}^*))_j\| \|\hat{\mathbf{H}} - \mathbf{H}^*\|_2 \leq \|(\mathcal{M}_3(\mathcal{B}^*))_j\| (\|\hat{\mathbf{H}}\|_2 + \|\mathbf{H}^*\|_2) \\
&\stackrel{(b)}{\leq} 2\|(\mathcal{M}_3(\mathcal{B}^*))_j\|,
\end{aligned} \tag{16}$$

where (a) follows from the Cauchy-Schwarz inequality, (b) comes from the fact that $\|\hat{\mathbf{H}}\|_2 = \|\mathbf{H}^*\|_2 = 1$ for the column-orthogonal matrices $\hat{\mathbf{H}}$ and \mathbf{H}^* . Setting $\bar{\alpha} = \max\{\|\mathbf{B}_j^*\|_F, j \in [p]\}$, we know that $(\nu_j - \mu_j)^2 \leq 4\bar{\alpha}^2$. Combining with (15) and (16), we obtain

$$\begin{aligned}
\mathbb{E}\|\boldsymbol{\phi}_{[1:s]} - \boldsymbol{\mu}_{[1:s]}\|^2 &= \mathbb{E}\left[\sum_{j=1}^s (\phi_j - \mu_j)^2\right] \leq \mathbb{E}\left[\sum_{j=1}^s (4\psi_j^2 + 8\bar{\alpha}^2)\right] \\
&= 8s\bar{\alpha}^2 + 4\mathbb{E}(\zeta^2) = 4s(2\bar{\alpha}^2 + K),
\end{aligned} \tag{17}$$

where $\zeta^2 = \sum_{j=1}^s \psi_j^2 \sim \chi_{sK}^2$. Therefore, combining with (13), (14) and (17) yields that

$$\begin{aligned}
E1 &\leq (1 + o(1))2\sigma^2 s \log(p/s) + 4s(2\bar{\alpha}^2 + K) \\
&\quad + 2\sqrt{4s(2\bar{\alpha}^2 + K)}\sqrt{(1 + o(1))2\sigma^2 s \log(p/s)} \\
&\sim (1 + o(1))2\sigma^2 s \log(p/s),
\end{aligned} \tag{18}$$

where the last step makes use of $s/p \rightarrow 0$.

We claim that $E2 = o(1)2\sigma^2 s \log(p/s)$ in the following. Note that $|\phi_j| = |\psi_j| \sim \chi_K$ since $\nu_j = 0$ for $j > s$. Denote $|\psi|_{(1)} \geq \cdots \geq |\psi|_{(p-s)}$ as the order statistics of $|\psi_{s+1}|, \dots, |\psi_p|$. It follows from the proof of Lemma 3.3 in Su & Candès (2016) that

$$\mathbb{E}\left[\sum_{j=s+1}^p \hat{\eta}_j^2\right] \leq \sum_{j=1}^{p-s} \mathbb{E}(|\psi|_{(j)} - \lambda_{s+j})_+^2,$$

where $x_+ = \max\{0, x\}$. Then, we can partition the sum into three parts

$$\sum_{j=1}^{p-s} \mathbb{E}(|\psi|_{(j)} - \lambda_{s+j})_+^2 = \sum_{j=1}^{\lfloor As \rfloor} \mathbb{E}(|\psi|_{(j)} - \lambda_{s+j})_+^2 + \sum_{j=\lceil As \rceil}^{\lfloor ap \rfloor} \mathbb{E}(|\psi|_{(j)} - \lambda_{s+j})_+^2 + \sum_{j=\lceil ap \rceil}^{p-s} \mathbb{E}(|\psi|_{(j)} - \lambda_{s+j})_+^2,$$

for a sufficiently large constant $A > 0$ and a sufficiently small constant $a > 0$. Note that Lemmas F.1, F.2 and F.3 given by Brzyski et al. (2019) show that each part is negligible compared with $2\sigma^2 s \log(p/s)$. This indicates that $E2 = o(1)2\sigma^2 s \log(p/s)$ and consequently completes the proof together with (18). \square

Remark 2 Note that a line of work on sparse and low-rank tensor regression has studied the minimax optimal rate of estimation errors, see, e.g., Hao et al. (2020), Raskutti et al. (2019), which give that

$$\inf_{\tilde{\mathcal{B}}} \sup_{\mathcal{B}^* \in \mathbb{B}_s} \mathbb{E} \|\tilde{\mathcal{B}} - \mathcal{B}^*\|_F^2 \asymp s \log(p/s),$$

where the infimum is taken over all estimators $\tilde{\mathcal{B}}$. Thus, together with (11), we have

$$\sup_{\mathcal{B}^* \in \mathbb{B}_s} \mathbb{E} \|\llbracket \hat{\mathcal{B}} \rrbracket_F - \llbracket \mathcal{B}^* \rrbracket_F\|^2 \sim \inf_{\tilde{\mathcal{B}}} \sup_{\mathcal{B}^* \in \mathbb{B}_s} \mathbb{E} \|\tilde{\mathcal{B}}_F - \mathcal{B}_F^*\|^2,$$

which indicates that our TgSLOPE estimator also enjoys the asymptotically minimax rate with respect to the ℓ_2 -loss at the frontal slice level.

4 Proximal DCA with Extrapolation

In this section, we propose a proximal difference-of-convex algorithm with extrapolation (pDCAe) to solve the TgSLOPE optimization problem and establish its global convergence.

4.1 DC Reformulation

Given an optimal solution $(\hat{\mathbf{G}}, \hat{\mathbf{H}})$ of the problem (4), it is known from the orthogonal Procrustes problem (Gower & Dijksterhuis 2004) that $\hat{\mathbf{H}}$ can be determined by $\hat{\mathbf{G}}$ in the way that $\hat{\mathbf{H}} = \hat{\mathbf{U}}_{[:,1:K]} \hat{\mathbf{V}}^T$, where $\hat{\mathbf{U}}, \hat{\mathbf{V}}$ are obtained from the SVD $\mathcal{M}_3(\mathcal{Y})^T \mathbf{X} \hat{\mathbf{G}} = \hat{\mathbf{U}} \mathbf{D} \hat{\mathbf{V}}^T$ with $\hat{\mathbf{U}} \in \mathbb{R}^{p_1 p_2 \times p_1 p_2}$, $\mathbf{D} \in \mathbb{R}^{p_1 p_2 \times K}$ and $\hat{\mathbf{V}} \in \mathbb{R}^{K \times K}$. Plugging $(\hat{\mathbf{G}}, \hat{\mathbf{H}})$ into the objective function of problem (4), we obtain that

$$\begin{aligned} L(\hat{\mathbf{G}}, \hat{\mathbf{H}}) &= \frac{1}{2} \|\mathcal{M}_3(\mathcal{Y})\|_F^2 + \frac{1}{2} \|\mathbf{X} \hat{\mathbf{G}} \hat{\mathbf{H}}^T\|_F^2 - \text{tr}(\mathcal{M}_3(\mathcal{Y})^T \mathbf{X} \hat{\mathbf{G}} \hat{\mathbf{H}}^T) \\ &= \frac{1}{2} \|\mathcal{M}_3(\mathcal{Y})\|_F^2 + \frac{1}{2} \|\mathbf{X} \hat{\mathbf{G}}\|_F^2 - \text{tr}(\mathbf{D} \hat{\mathbf{U}}_{[:,1:K]}^T \hat{\mathbf{U}}) \\ &= \frac{1}{2} \|\mathcal{M}_3(\mathcal{Y})\|_F^2 + \frac{1}{2} \|\mathbf{X} \hat{\mathbf{G}}\|_F^2 - \text{tr}(\mathbf{D}) \\ &= \frac{1}{2} \|\mathcal{M}_3(\mathcal{Y})\|_F^2 + \frac{1}{2} \|\mathbf{X} \hat{\mathbf{G}}\|_F^2 - \|\mathcal{M}_3(\mathcal{Y})^T \mathbf{X} \hat{\mathbf{G}}\|_*. \end{aligned}$$

Therefore, the TgSLOPE problem (4) can be equivalently transformed into

$$\begin{cases} \hat{\mathbf{G}} = \arg \min \left\{ F(\mathbf{G}) = \frac{1}{2} \|\mathbf{X} \mathbf{G}\|_F^2 + P_\lambda(\llbracket \mathbf{G} \rrbracket) - \|\mathcal{M}_3(\mathcal{Y})^T \mathbf{X} \mathbf{G}\|_* \right\}, \\ \hat{\mathbf{H}} = \hat{\mathbf{U}}_{[:,1:K]} \hat{\mathbf{V}}^T, \text{ where } \hat{\mathbf{U}} \text{ and } \hat{\mathbf{V}} \text{ are from the SVD } \mathcal{M}_3(\mathcal{Y})^T \mathbf{X} \hat{\mathbf{G}} = \hat{\mathbf{U}} \mathbf{D} \hat{\mathbf{V}}^T. \end{cases} \quad (19)$$

Denote $F1(\mathbf{G}) = \frac{1}{2} \|\mathbf{X} \mathbf{G}\|_F^2$ and $F2(\mathbf{G}) = \frac{L}{2} \|\mathbf{G}\|_F^2 - F1(\mathbf{G})$. Since $F1$ is gradient Lipschitz continuous with modulus $L = \|\mathbf{X}^T \mathbf{X}\|_2$, the convexity of $F2$ follows. Inspired by the DC-representable function from Gotoh et al. (2018), we rewrite the optimization problem in (19) as

$$\min_{\mathbf{G} \in \mathbb{R}^{p \times K}} F(\mathbf{G}) = \underbrace{\frac{L}{2} \|\mathbf{G}\|_F^2 + P_\lambda(\llbracket \mathbf{G} \rrbracket)}_{C1(\mathbf{G})} - \underbrace{\left(\frac{L}{2} \|\mathbf{G}\|_F^2 - \frac{1}{2} \|\mathbf{X} \mathbf{G}\|_F^2 + N(\mathbf{G}) \right)}_{C2(\mathbf{G})}, \quad (20)$$

where $N(\mathbf{G}) = \|\mathcal{M}_3(\mathcal{Y})^\top \mathbf{X} \mathbf{G}\|_*$. It is easy to verify that both $C1$ and $C2$ are convex, leading to a DC program as in (20).

By now, we constructively reformulate the manifold optimization problem (4) as a DC program (20). This allows us to solve the reformulation problem of TgSLOPE by a DC-type algorithm.

4.2 Proximal DCA

Considering the DC program (20), we first give the subdifferential of $N(\mathbf{G})$ in the following lemma, which can be clearly derived from the subdifferential of the matrix nuclear norm (Watson 1992) and the chain rule of Theorem 10.6 in Rockafellar & Wets (2009).

Lemma 2 *The subdifferential of $N(\mathbf{G})$ is given by*

$$\partial N(\mathbf{G}) = \{\mathbf{X}^\top \mathcal{M}_3(\mathcal{Y})(\tilde{\mathbf{U}}_{[:,1:K]} \tilde{\mathbf{V}}^\top + \tilde{\mathbf{W}}) : \tilde{\mathbf{U}}_{[:,1:K]}^\top \tilde{\mathbf{W}} = \mathbf{O}, \tilde{\mathbf{W}} \tilde{\mathbf{V}} = \mathbf{O}, \|\tilde{\mathbf{W}}\|_2 \leq 1\}, \quad (21)$$

where $\tilde{\mathbf{U}}, \tilde{\mathbf{V}}$ are obtained by the SVD of $\mathcal{M}_3(\mathcal{Y})^\top \mathbf{X} \mathbf{G} = \tilde{\mathbf{U}} \mathbf{D} \tilde{\mathbf{V}}^\top$.

The DCA iterative scheme for (20) takes the following form

$$\begin{aligned} \mathbf{G}^{(k+1)} &= \arg \min_{\mathbf{G}} \left\{ \frac{L}{2} \|\mathbf{G}\|_F^2 - \langle \mathbf{G}, (L\mathbf{I} - \mathbf{X}^\top \mathbf{X}) \mathbf{G}^{(k)} + \mathbf{Q}_1^{(k)} \rangle + P_\lambda(\llbracket \mathbf{G} \rrbracket) \right\} \\ &= \arg \min_{\mathbf{G}} \left\{ \frac{1}{2} \left\| \mathbf{G} - \left(\mathbf{G}^{(k)} - \frac{1}{L} (\mathbf{X}^\top \mathbf{X} \mathbf{G}^{(k)} - \mathbf{Q}_1^{(k)}) \right) \right\|_F^2 + P_{\lambda/L}(\llbracket \mathbf{G} \rrbracket) \right\}, \end{aligned} \quad (22)$$

where $\mathbf{Q}_1^{(k)} \in \partial N(\mathbf{G}^{(k)})$. Then the optimal solution of problem (22) can be computed by the proximal operator of the penalty function $P_{\lambda/L}$. Specifically,

$$\begin{cases} \boldsymbol{\eta}^{(k+1)} = \arg \min_{\boldsymbol{\eta}} \left\{ \frac{1}{2} \|\llbracket \mathbf{Q}^{(k)} \rrbracket - \boldsymbol{\eta}\|^2 + P_{\lambda/L}(\boldsymbol{\eta}) \right\}, \\ \mathbf{g}_j^{(k+1)} = (\text{Prox}_{P_{\lambda/L}}(\mathbf{Q}^{(k)}))_j = \eta_j^{(k+1)} \frac{\mathbf{q}_j^{(k)}}{\|\mathbf{q}_j^{(k)}\|}, j \in [p], \end{cases} \quad (23)$$

where $\mathbf{Q}^{(k)} = \mathbf{G}^{(k)} - (\mathbf{X}^\top \mathbf{X} \mathbf{G}^{(k)} - \mathbf{Q}_1^{(k)})/L$. The resulting DCA is called as the proximal DCA (Gotoh et al. 2018, Wen et al. 2018). Consequently, the \mathbf{G} -subproblem is reduced to identifying the general SLOPE proximal operator, which can be efficiently solved by FastProxSL1 (Bogdan et al. 2015). Furthermore, in order to possibly accelerate the algorithm, we entertain extrapolation techniques (Nesterov 2013) in the proximal DCA. The algorithmic framework is summarized in Algorithm 1.

Note that the pDCAe algorithm is reduced to the general proximal DCA if $\beta^{(k)} = 0$ for all k . Moreover, Algorithm 1 can be coupled with many popular choices of extrapolation parameters $\{\beta^{(k)}\}$ including that used in accelerated proximal gradient (APG) for solving SLOPE (Bogdan et al. 2015). In our numerical experiments section, we follow Bogdan et al. (2015) and set $\theta^{(-1)} = 1$,

$$\beta^{(k)} = \frac{\theta^{(k-1)} - 1}{\theta^{(k)}} \quad \text{with} \quad \theta^{(k)} = \frac{1 + \sqrt{1 + 4(\theta^{(k-1)})^2}}{2}, \quad \forall k \geq 0.$$

Algorithm 1 pDCAe for solving TgSLOPE (4)

Initialize $\mathbf{G}^{(0)} \in \mathbb{R}^{p \times K}$, $\{\beta^{(k)}\} \subseteq [0, 1)$ with $\sup_k \beta^{(k)} < 1$, set $\mathbf{G}^{(-1)} = \mathbf{G}^{(0)}$, $k = 0$;

- 1: Choose $\mathbf{Q}_1^{(k)} \in \partial N(\mathbf{G}^{(k)})$ by (21);
- 2: Compute $\mathbf{A}^{(k)} = \mathbf{G}^{(k)} + \beta^{(k)}(\mathbf{G}^{(k)} - \mathbf{G}^{(k-1)})$ and update

$$\mathbf{Q}^{(k)} = \mathbf{A}^{(k)} - (\mathbf{X}^\top \mathbf{X} \mathbf{A}^{(k)} - \mathbf{Q}_1^{(k)})/L;$$

- 3: Compute $\mathbf{G}^{(k+1)}$ by the two-step form in (23);
- 4: Set $k = k + 1$. If the stopping criterion is met, perform the SVD $\mathcal{M}_3(\mathcal{Y})^\top \mathbf{X} \mathbf{G}^{(k)} = \mathbf{U}^{(k)} \mathbf{D}^{(k)} \mathbf{V}^{(k)\top}$ to get

$$\mathbf{H}^{(k)} = (\mathbf{U}^{(k)})_{[:,1:K]} \mathbf{V}^{(k)\top},$$

then stop and return $\mathcal{B}^{(k)} = \mathcal{M}_3^{-1}(\mathbf{G}^{(k)} \mathbf{H}^{(k)\top})$; otherwise, go to the step 1.

4.3 Global Convergence

This subsection is dedicated to the global convergence for pDCAe. We start with the level-coercivity of the DC function $F(\mathbf{G})$.

Lemma 3 *Let the predictor matrix \mathbf{X} in the TgSLOPE problem (4) be full column rank. Then the DC function $F(\mathbf{G})$ in (20) is level-coercive in the sense that $\liminf_{\|\mathbf{G}\|_F \rightarrow \infty} \frac{F(\mathbf{G})}{\|\mathbf{G}\|_F} > 0$.*

Proof. Denoting $\sigma_1 \geq \sigma_2 \geq \dots \geq \sigma_K$ as singular values of \mathbf{G} , we can obtain that

$$\|\mathbf{G}\|_*^2 = \left(\sum_{i=1}^K \sigma_i \right)^2 \leq K \sum_{i=1}^K \sigma_i^2 = K \|\mathbf{G}\|_F^2. \quad (24)$$

In addition, we know from the singular value inequality (Chatelin 1983) that $\sigma_{i+j-1}(\mathbf{AB}) \leq \sigma_i(\mathbf{A})\sigma_j(\mathbf{B})$ for $1 \leq i, j \leq K, i+j \leq K+1$, which implies that $\|\mathbf{AB}\|_* \leq \|\mathbf{A}\|_* \|\mathbf{B}\|_*$ for any two matrices $\mathbf{A} \in \mathbb{R}^{p_1 p_2 \times p}$ and $\mathbf{B} \in \mathbb{R}^{p \times K}$. Together with (24), we derive that as $\|\mathbf{G}\|_F \rightarrow \infty$,

$$\begin{aligned} \frac{F(\mathbf{G})}{\|\mathbf{G}\|_F} &= \frac{\|\mathbf{XG}\|_F^2/2 + P_\lambda(\|\mathbf{G}\|) - \|\mathcal{M}_3(\mathcal{Y})^\top \mathbf{XG}\|_*}{\|\mathbf{G}\|_F} \\ &\geq \frac{\|\mathbf{XG}\|_F^2/2 + P_\lambda(\|\mathbf{G}\|)}{\|\mathbf{G}\|_F} - \frac{\|\mathcal{M}_3(\mathcal{Y})^\top \mathbf{X}\|_* \|\mathbf{G}\|_*}{\|\mathbf{G}\|_F} \\ &\geq \frac{\|\mathbf{XG}\|_F^2/2 + P_\lambda(\|\mathbf{G}\|)}{\|\mathbf{G}\|_F} - \sqrt{K} \|\mathcal{M}_3(\mathcal{Y})^\top \mathbf{X}\|_* \rightarrow \infty, \end{aligned}$$

where ‘ \rightarrow ’ is from the fact that the inequality $\|\mathbf{XG}\|_F^2 \geq \sigma_p^2(\mathbf{X})\|\mathbf{G}\|_F^2$ holds with $\sigma_p(\mathbf{X}) > 0$ when \mathbf{X} is full column rank. This completes the proof. \square

Theorem 3 *Let $\{\mathbf{G}^{(k)}\}$ be the sequence generated by Algorithm 1 for solving problem (4). Then the following properties hold:*

- (a) *The sequence $\{\mathbf{G}^{(k)}\}$ is bounded;*
- (b) *$\lim_{k \rightarrow \infty} \|\mathbf{G}^{(k+1)} - \mathbf{G}^{(k)}\|_F = 0$;*

(c) Every limit point $\bar{\mathbf{G}}$ of the sequence $\{\mathbf{G}^{(k)}\}$ is a stationary point of F in the sense that

$$\mathbf{0} \in \mathbf{X}^T \mathbf{X} \bar{\mathbf{G}} + \partial P_\lambda(\llbracket \bar{\mathbf{G}} \rrbracket) - \partial \|\mathcal{M}_3(\mathcal{Y})^T \mathbf{X} \bar{\mathbf{G}}\|_*.$$

Proof. It follows from Lemma 3 that the DC function F in (20) is also level-bounded, that is, the level set $L_\alpha = \{\mathbf{G} \in \mathbb{R}^{p \times K} : F(\mathbf{G}) \leq \alpha\}$ is bounded for any $\alpha \in \mathbb{R}$. In addition, we know from Wen et al. (2018) that pDCAe enjoys the global convergence if F is level-bounded. Thus, using Lemma 3, the desired properties in (a)-(c) are consequences of Theorem 4.1 in Wen et al. (2018). \square

As shown in (b) of the above convergence results, we take a reasonable termination criterion for Algorithm 1 that

$$\frac{\|\mathbf{G}^{(k)} - \mathbf{G}^{(k-1)}\|_F}{\max\{\|\mathbf{G}^{(k-1)}\|_F, 1\}} \leq \epsilon$$

for some given parameter $\epsilon > 0$.

Remark 3 Let $\bar{\mathbf{G}}$ be the limit point of the sequence $\{\mathbf{G}^{(k)}\}$ generated by Algorithm 1, and $\bar{\mathbf{H}} = \bar{\mathbf{U}}_{[:,1:K]} \bar{\mathbf{V}}^T$, where $\bar{\mathbf{U}}$ and $\bar{\mathbf{V}}$ are from the SVD $\mathcal{M}_3(\mathcal{Y})^T \mathbf{X} \bar{\mathbf{G}} = \bar{\mathbf{U}} \bar{\mathbf{D}} \bar{\mathbf{V}}^T$. It is easily verified that the linear independence constraint qualification (LICQ) (Bertsekas 1999) is satisfied for $\mathbf{H}^T \mathbf{H} = \mathbf{I}_K$. Thus, together with Theorem 3, $(\bar{\mathbf{G}}, \bar{\mathbf{H}})$ is a stationary point of the TgSLOPE problem (4) in the sense that

$$\begin{cases} \mathbf{0} \in \mathbf{X}^T (\mathcal{M}(\mathcal{Y}) - \mathbf{X} \bar{\mathbf{G}} \bar{\mathbf{H}}^T) \bar{\mathbf{H}} + \partial P_\lambda(\llbracket \bar{\mathbf{G}} \rrbracket), \\ \mathbf{0} = (\mathcal{M}(\mathcal{Y}) - \mathbf{X} \bar{\mathbf{G}} \bar{\mathbf{H}}^T)^T \mathbf{X} \bar{\mathbf{G}} + 2 \bar{\mathbf{H}} \boldsymbol{\Lambda} \text{ with } \boldsymbol{\Lambda} \in \mathbb{R}^{K \times K}. \end{cases}$$

5 Numerical Experiments

This section gives some experiments on synthetic data and a real human brain connection data. All numerical experiments are implemented in MATLAB (R2021a), running on a laptop with Intel Core i5-8265U CPU (1.60GHz) and 16 GB RAM.

5.1 Comparative Methods

We verify performances of the proposed TgSLOPE by comparing it with the following three approaches:

(a) TBMM: the block majorization minimization (BMM) algorithm proposed by Wei et al. (2021) to solve the TgSLOPE problem (4), whose corresponding iterative scheme is

$$\begin{cases} \mathbf{G}^{(k+1)} = \arg \min_{\mathbf{G}} \left\{ \frac{1}{2} \|\mathbf{G} - \mathbf{R}^{(k)}\|_F^2 + P_{\lambda/L}(\llbracket \mathbf{G} \rrbracket) \right\}, \\ \mathbf{H}^{(k+1)} = (\mathbf{U}^{(k+1)})_{[:,1:K]} \mathbf{V}^{(k+1)T}, \end{cases}$$

where $\mathbf{R}^{(k)} = \mathbf{G}^{(k)} - (\mathbf{X}^T \mathbf{X} \mathbf{G}^{(k)} - \mathbf{X}^T \mathcal{M}_3(\mathcal{Y}) \mathbf{H}^{(k)})/L$, $\mathbf{U}^{(k+1)}$ and $\mathbf{V}^{(k+1)}$ are from the SVD $\mathcal{M}_3(\mathcal{Y})^T \mathbf{X} \mathbf{G}^{(k+1)} = \mathbf{U}^{(k+1)} \mathbf{D}^{(k+1)} \mathbf{V}^{(k+1)T}$;

(b) TgLASSO: the group LASSO penalized CP low-rank tensor regression approach, in which the pDCAe algorithm in Section 4 is used to solve

$$\min_{\mathbf{G}, \mathbf{H}} \left\{ \frac{1}{2} \|\mathcal{M}_3(\mathcal{Y}) - \mathbf{X} \mathbf{G} \mathbf{H}^T\|_F^2 + \lambda \sum_{j=1}^p \|\mathbf{g}_j\| : \mathbf{H}^T \mathbf{H} = \mathbf{I}_K \right\},$$

where the tuning parameter $\lambda > 0$ is selected by 5-fold cross-validation;

(c) TLRR: the CP low-rank tensor regression (without sparse penalty), in which the pDCAe is applied to solve

$$\min_{\mathbf{G}, \mathbf{H}} \left\{ \frac{1}{2} \left\| \mathcal{M}_3(\mathcal{Y}) - \mathbf{X} \mathbf{G} \mathbf{H}^T \right\|_F^2 : \mathbf{H}^T \mathbf{H} = \mathbf{I}_K \right\}.$$

5.2 Synthetic Data

In our numerical experiments on synthetic data, we adopt the measures including TgFDR defined in (5) and the tensor power (TP) to evaluate selection performances of the estimator $\hat{\mathcal{B}}$ generated by a given method. Here TP is defined as

$$\text{TP} = \mathbb{E}(T)/s, \text{ where } T = \#\{j \in [p] : \mathbf{B}_j^* \neq \mathbf{O}, \hat{\mathbf{B}}_j \neq \mathbf{O}\} \text{ and } s = \#\{j \in [p] : \mathbf{B}_j^* \neq \mathbf{O}\}.$$

For estimation accuracy, we evaluate the performance of $\hat{\mathcal{B}}$ in terms of the relative group estimate error (RgEE) and the mean squared error (MSE) defined respectively as

$$\text{RgEE} = \frac{\|[\hat{\mathcal{B}}]_F - [\mathcal{B}^*]_F\|^2}{\|[\mathcal{B}^*]_F\|^2}, \quad \text{MSE} = \|(\hat{\mathcal{B}} - \mathcal{B}^*) \times_3 \mathbf{X}\|_F^2 / np_1 p_2.$$

Meanwhile, to evaluate the time efficiency of our proposed pDCAe algorithm, the CPU time (Time) is reported for each testing instance.

The predictor matrix $\mathbf{X} \in \mathbb{R}^{n \times p}$ is generated in the following two cases:

- (a) Orthogonal design with $n = p$, where the orthogonal matrix \mathbf{X} is generated from the QR factorization of a $n \times n$ matrix with i.i.d. standard normal distributed entries;
- (b) Gaussian random design, where the entries of \mathbf{X} are i.i.d. drawn from $N(0, 1/n)$.

In addition, the ground truth is simulated via $\mathcal{B}^* = \mathcal{M}_3^{-1}(\mathbf{G}^* \mathbf{H}^{*T}) \in \mathbb{R}^{p_1 \times p_2 \times p}$, in which $\mathbf{G}^* \in \mathbb{R}^{p \times K}$ is generated in a similar manner as in Brzyski et al. (2019) with s nonzero rows, $\mathbf{H}^* \in \mathbb{R}^{p_1 p_2 \times K}$ is column-orthogonal. Specifically, each nonzero row of \mathbf{G}^* is generated from the uniform distribution $U[0.1, 1.1]$ and then we scale it such that $\|\mathbf{g}_j^*\| = a\sqrt{K}$ with $a = \sqrt{4 \ln(p)/(1 - p^{-2/K}) - K}$. The matrix \mathbf{H}^* is simulated as the first K left singular vectors of a $p_1 p_2 \times p_1 p_2$ matrix with i.i.d. standard normal distributed entries. The response tensor $\mathcal{Y} \in \mathbb{R}^{p_1 \times p_2 \times n}$ is simulated by $\mathcal{Y} = \mathcal{B}^* \times_3 \mathbf{X} + \mathcal{E}$, where the entries of the noise tensor \mathcal{E} are i.i.d. drawn from $N(0, 1)$.

To verify the TgFDR controlling performance of TgSLOPE, we first consider the orthogonal design situation of \mathbf{X} . Set $n = p = 1000, p_1 = p_2 = 10, K = 20$ and sparsity $s = 25 : 25 : 250$. We perform 100 independent replications for each sparsity and target TgFDR level ($q = 0.05, 0.1$). As shown in Figure 4 (a), for all testing instances, TgSLOPE maintains a comparable TgFDR with the ‘nominal’ level when it works with the regularization parameter vector $\boldsymbol{\lambda}$ shown in Figure 4 (b). In addition, TgSLOPE reports the estimated tensor power $\text{TP} = 1$ for all cases.

In the following numerical comparisons, we consider the Gaussian random situation and test the effect of sparsity s , model size p and CP rank K respectively under the target TgFDR level $q = 0.05$. For TgSLOPE, we select its regularization parameters according to Procedure 2 of Brzyski et al. (2019).

(a) Sparsity effect. Set $n = 3000, p = 1000, p_1 = p_2 = 10$ and $K = 20$. We test performances of four approaches under various sparsity with $s = 25 : 25 : 250$. Simulation results report $\text{TP} = 1$

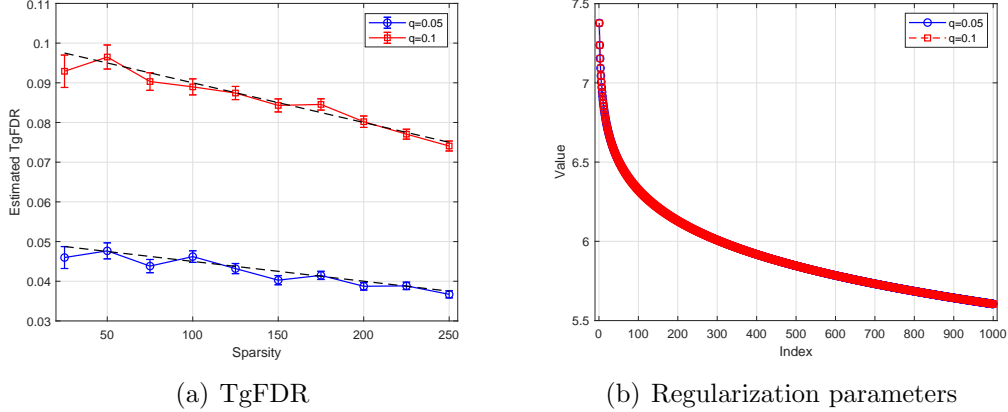


Figure 4: Estimated TgFDR and selected regularization parameters with $n = p = 1000, p_1 = p_2 = 10, K = 20$ under the orthogonal situation of the matrix \mathbf{X} . In (a), bars correspond to \pm SE (standard error), black dotted lines represent the ‘nominal’ TgFDR level $q \cdot (p - s)/p$. In (b), the regularization parameter vector λ follows the definition in (7).

for all competitors in each testing instance. In addition, average results based on 100 independent replications have been shown in Figure 5. (i) Figure 5 (a) illustrates that TgSLOPE and TBMM have significant superiority in terms of TgFDR, with TgFDR below ‘nominal’ for all testing sparsity. (ii) TgLASSO fails to control TgFDR, although it reports the relatively small RgEE and MSE as shown in Figure 5 (b) and (c). (iii) Figure 5 (d) shows that TgSLOPE reports a relatively short CUP time, especially in the cases of small sparsity. (iv) It is intuitive that those four methods tend to have comparable performances as the sparsity increases.

(b) Model size effect. In this example, we test the effect of model size p comparing among four approaches. Set $n = 3000, p_1 = p_2 = 10, K = 20$ and the sparsity $s = 0.02p$ with model size $p = 2000, 4000, 6000$. In each testing instance, all these competitors report TP = 1. Moreover, Table 1 collects the average results based on 100 independent replications for each model size. (i) As suggested in Table 1, TLRR gives the worst performances. For the other three approaches, all of the four evaluation metrics tend to become larger as the model size grows. (ii) Similar to the results shown in Figure 5, TgLASSO fails to control TgFDR, while TgSLOPE and TBMM can maintain the TgFDR below the ‘nominal’ TgFDR level for all testing model sizes, with predictable sacrifice on the estimation accuracy. (iii) We can also see from Table 1 that TgSLOPE gives the smaller TgFDR than TBMM for the model size $p = 6000$, and it reports the least CPU time for all cases.

(c) CP rank effect. We now examine the impact of CP rank on the four approaches under $p_1 = p_2 = 10$ and $p_1 = p_2 = 20$, respectively. Set $n = 1000, p = 2000$ and the sparsity $s = 0.02p$. It is known from Kolda & Bader (2009) that CP rank $K \leq \{p_1 p_2, p p_1, p p_2\}$, then we set CP rank $K = 5 : 5 : 50$. All testing instances are simulated based on 100 independent replications. Simulation results report that TP = 1 for all the competitors. Figure 6 depicts changes of the four evaluation metrics with the increase of CP rank. (i) Our proposed TgSLOPE procedure works well in terms of TgFDR, especially for small CP ranks. See, e.g., as shown in Figure 6 (a) and (b), TgSLOPE and TBMM report the lower TgFDR than the ‘nominal’ level as $K \leq 25$. (ii) Figure 6 (g) and (h) illustrate that TgSLOPE reports a relatively short CPU time, especially compared

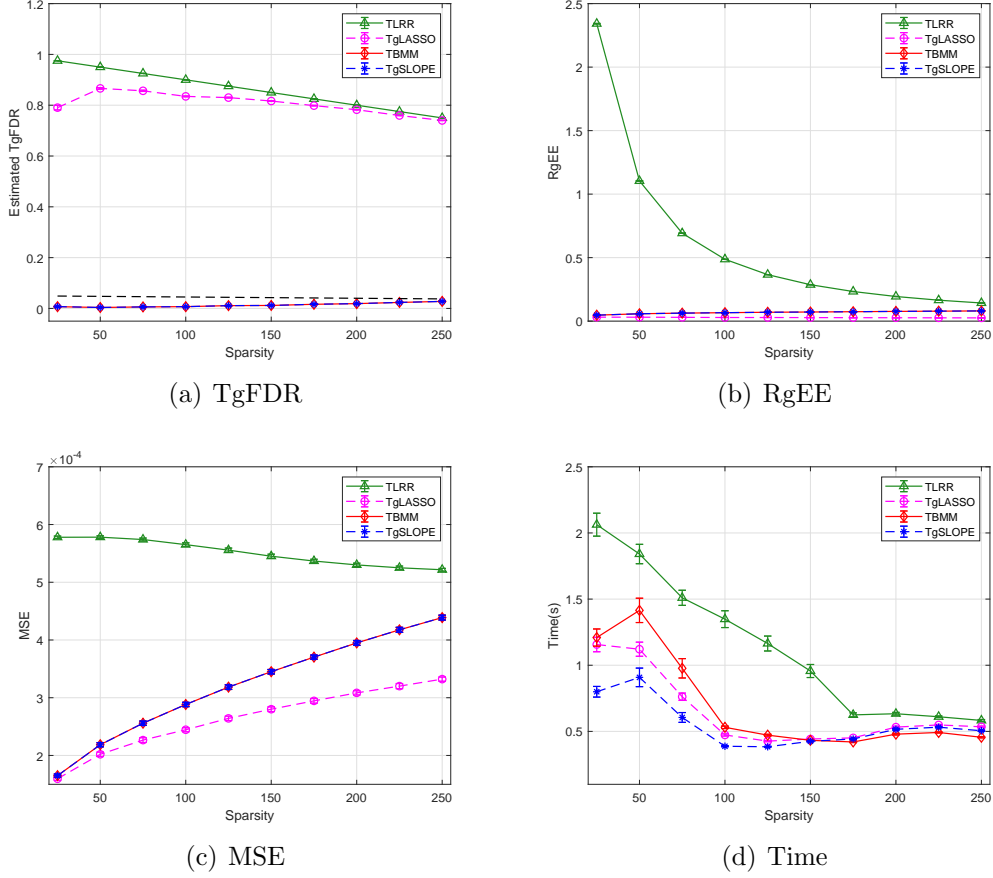


Figure 5: Average results with various sparsity under $n = 3000, p = 1000, p_1 = p_2 = 10, K = 20$ and for the Gaussian random design situation of \mathbf{X} . Bars correspond to \pm SD (standard deviation). In (a), black dotted lines represent the ‘nominal’ TgFDR level $q \cdot (p - s)/p$.

Table 1: Average results with different model size under $n = 3000, p_1 = p_2 = 10, K = 20, s = 0.02p$ for the Gaussian random design situation of \mathbf{X} . Standard deviations are presented in brackets.

Size	Method	TgFDR	RgEE	MSE	Time(s)
$p = 2000$	TLRR	0.980	5.10e-0 (6.24e-2)	7.77e-4 (1.89e-6)	3.325
	TgLASSO	0.891	3.44e-2 (3.97e-3)	1.92e-4 (4.45e-6)	1.566
	TBMM	0.006	5.59e-2 (3.91e-3)	2.02e-4 (2.73e-6)	2.242
	TgSLOPE	0.007	5.59e-2 (3.91e-3)	2.02e-4 (2.76e-6)	1.081
$p = 4000$	TLRR	0.980	3.92e-0 (4.26e-2)	9.28e-4 (2.45e-6)	10.163
	TgLASSO	0.921	3.50e-2 (2.16e-3)	2.40e-4 (4.70e-6)	3.727
	TBMM	0.008	6.46e-2 (3.28e-3)	2.70e-4 (3.48e-6)	6.104
	TgSLOPE	0.008	6.45e-2 (3.27e-3)	2.70e-4 (3.49e-6)	2.962
$p = 6000$	TLRR	0.980	1.69e-0 (1.71e-2)	9.19e-4 (2.94e-6)	15.146
	TgLASSO	0.924	3.66e-2 (2.17e-3)	2.77e-4 (5.16e-6)	6.179
	TBMM	0.025	6.91e-2 (3.78e-3)	3.24e-4 (4.02e-6)	9.108
	TgSLOPE	0.014	6.88e-2 (3.75e-3)	3.24e-4 (4.01e-6)	5.666

with TBMM. For example, as $p_1 = p_2 = 20$ and $K \leq 35$, the CPU time reported by TgSLOPE is no more than 1/5 of that of TBMM. (iii) For the fixed tensor size, we can see from Figure 6 (a) and (b) that the TgFDR tends to become larger as the CP rank increases. In addition, with the increase of the CP rank, Figure 6 (c) and (d) show that RgEE reduces, while Figure 6 (e) and (f) show that MSE grows. This may give us some inspiration to choose a moderate CP rank.

5.3 Human Brain Connection Data

In this subsection, we test our proposed TgSLOPE comparing with the other three approaches on a real human brain connection (HBC) data from the Human Connectome Project (HCP), which aims to build a network map between the anatomical and functional connectivity within healthy human brains (Van Essen et al. 2013).

The preprocessed HBC dataset is provided by Hu et al. (2022), in which the response is a 68×68 binary matrix with entries encoding the presence or absence of fiber connections between 68 brain regions-of-interest, the predictor matrix is collected from different personal features for each observed individual. After removing those missing values, the HBC dataset consists of 111 individuals and 549 personal features, including gender, age, etc. (The full list of features can be found at <https://wiki.humanconnectome.org/display/PublicData/>). For this real dataset analysis, the number of discovered features (Discovery), mean squared prediction error (MSPE) and CPU time are adopted to evaluate the performance of the four competitors. Here, Discovery and MSPE are defined respectively as

$$\begin{aligned} \text{Discovery} &= \#\{j \in [p] : (\hat{\mathbf{B}}_{\text{training}})_j \neq \mathbf{O}\}, \\ \text{MSPE} &= \|\mathcal{Y}_{\text{test}} - \hat{\mathbf{B}}_{\text{training}} \times_3 \mathbf{X}_{\text{test}}\|_F^2 / p_1 p_2 n_{\text{test}}, \end{aligned}$$

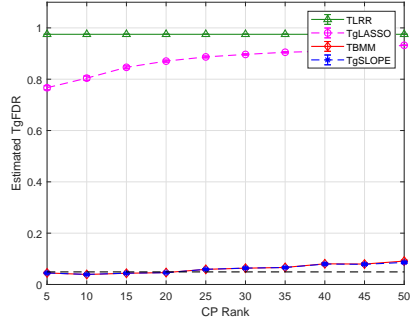
where $\hat{\mathbf{B}}_{\text{training}}$ is the estimator for the training set, \mathbf{X}_{test} , $\mathcal{Y}_{\text{test}}$ and n_{test} are the predictor matrix, response tensor and the sample size of the testing set, respectively.

We first test the performance of four approaches under different CP ranks. For each CP rank selected from 1 to 15, HBC dataset is randomly divided into 80 percent of training set and 20 percent of testing set 20 times. The average numerical results are collected in Figure 7. It is intuitive that all of the three evaluation metrics tend to be larger as the CP rank increases. We can also see from Figure 7 that TLRR fails to feature selection and gives the largest MSPE. In addition, Figure 7 (a) reports the fewest discovered features of TgSLOPE at the majority of CP ranks such as $K \leq 12$. Meanwhile, as Figure 7 (b) suggested, TgSLOPE gives the relatively less MSPE than TgLASSO for all testing instances. With respect to the CPU time, TgSLOPE has a significant superiority comparing with TBMM. See, e.g., as Figure 7 (c) shows, the reported time of TBMM is over six times longer than that of TgSLOPE.

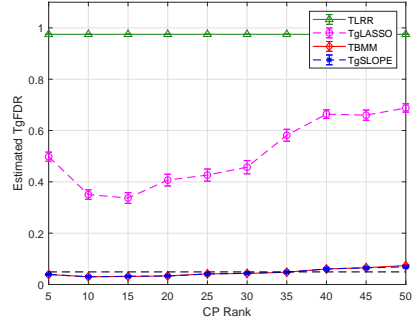
Next, we choose the combination of CP rank K and regularization parameters $\boldsymbol{\lambda}$ via a BIC-type criterion on the whole HBC dataset, which minimizes

$$\text{BIC} = \log(\|\mathcal{Y} - \hat{\mathbf{B}} \times_3 \mathbf{X}\|_F^2) + (\text{Discovery} + p_1 p_2) K \log(np_1 p_2).$$

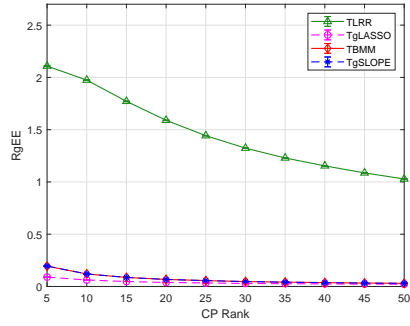
Figure 8 depicts the numerical results based on 20 independent replications. It reports the similar results to Figure 7. Overall, TgSLOPE gives the best performance, among the four competitors.



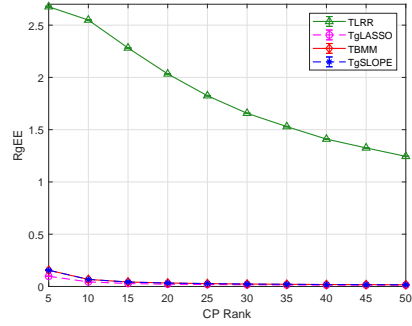
(a) TgFDR



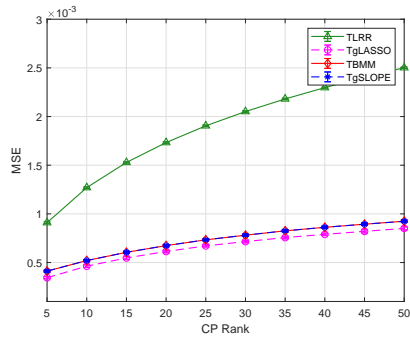
(b) TgFDR



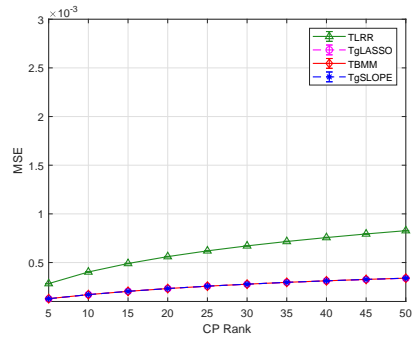
(c) RgEE



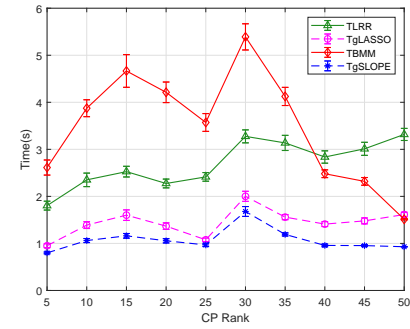
(d) RgEE



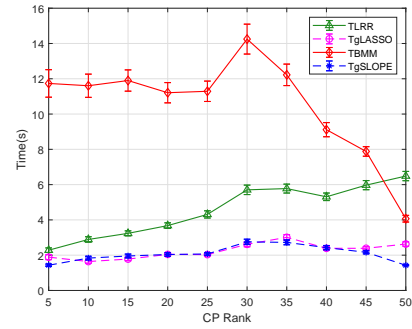
(e) MSE



(f) MSE



(g) Time



(h) Time

Figure 6: Simulation results with different CP rank under $n = 1000, p = 2000, s = 0.02p$ for the Gaussian random design situation of \mathbf{X} . Left column: $p_1 = p_2 = 10$, right column: $p_1 = p_2 = 20$. In (a) and (b), black dotted lines represent the ‘nominal’ TgFDR level $q \cdot (p - s)/p$.

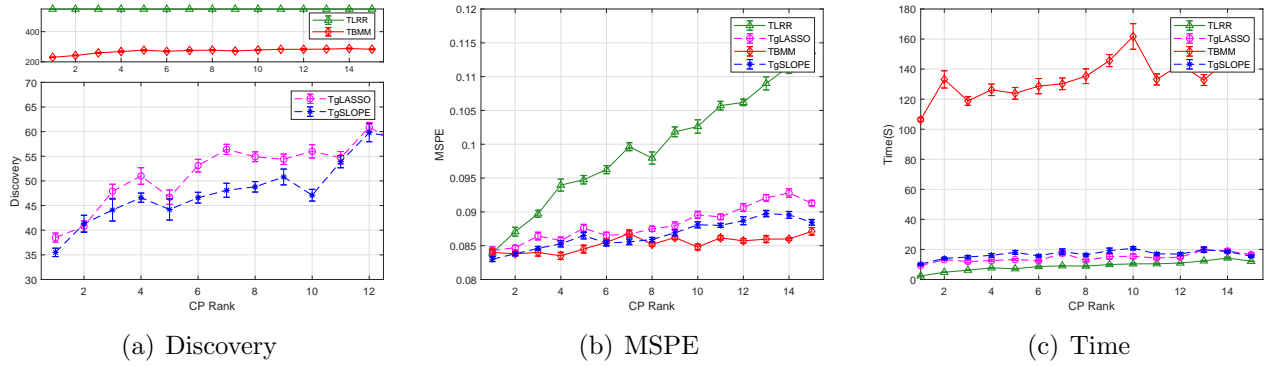


Figure 7: Average results with the different CP rank based on 20 randomly 8:2 splits for HBC dataset.

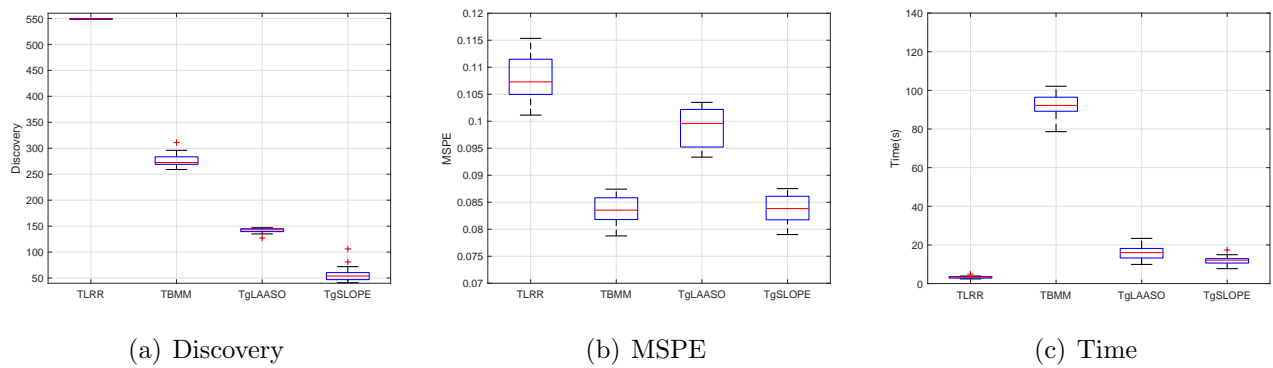


Figure 8: Average results with the BIC-type CP rank based on 20 randomly 8:2 splits for HBC dataset.

6 Conclusions

In this article we propose a sparse and low-rank tensor regression method, which optimizes a gSLOPE penalized CP low-rank tensor minimization problem. Under the assumption of column-orthogonality for the predictor matrix, we show that our proposed TgSLOPE procedure controls TgFDR at a pre-set level, and achieves the asymptotically minimax convergence with respect to the ℓ_2 -loss defined by frontal slices of the produced estimator. This provides theoretical guarantees for feature selection and coefficient estimation in finite samples. Moreover, a globally convergent pDCAe algorithm is applied to solve the TgSLOPE estimator by constructively reformulating our TgSLOPE problem into a DC program. Numerical experiments verify the superiority of our method in terms of TgFDR control, estimation accuracy and CPU time against three state-of-the-art approaches.

For the TgSLOPE method, it would be interesting to investigate statistical properties including TgFDR control and estimate accuracy in more general cases besides the orthogonal design. Moreover, Luo et al. (2019) propose a sparse semismooth Newton-based augmented Lagrangian method (Newt-ALM) to solve the SLOPE model of the classical linear regression (Bogdan et al. 2015) and show that Newt-ALM offers a notable computational advantage in the high-dimensional settings comparing with the first-order algorithms, such as APG and alternating direction method of multipliers (ADMM). How to design the robust and highly efficient Newton-type algorithm for TgSLOPE based models is also one of our research topic in the future.

Funding

This research was supported by Beijing Natural Science Foundation (grant number Z190002).

References

- Ahmed, T., Raja, H. & Bajwa, W. U. (2020), ‘Tensor Regression Using Low-Rank and Sparse Tucker Decompositions’, *SIAM Journal on Mathematics of Data Science* **2**(4), 944–966.
- Allen, G. I. (2012), Sparse Higher-Order Principal Components Analysis, *in* ‘Proceedings of the 15th International Conference on Artificial Intelligence and Statistics’, pp. 27–36.
- Bellec, P. C., Lecué, G. & Tsybakov, A. B. (2018), ‘SLOPE Meets LASSO: Improved Oracle Bounds and Optimality’, *The Annals of Statistics* **46**(6), 3603–3642.
- Benjamini, Y. & Hochberg, Y. (1995), ‘Controlling the False Discovery Rate: A Practical and Powerful Approach to Multiple Testing’, *Journal of the Royal Statistical Society, Series B* **57**(1), 289–300.
- Bertsekas, D. P. (1999), *Nonlinear Programming*, Athena Scientific.
- Bogdan, M., Van Den Berg, E., Sabatti, C., Su, W. & Candès, E. J. (2015), ‘SLOPE-Adaptive Variable Selection via Convex Optimization’, *Annals of Applied Statistics* **9**(3), 1103–1140.
- Brzyski, D., Gossman, A., Su, W. & Bogdan, M. (2019), ‘Group SLOPE-Adaptive Selection of Groups of Predictors’, *Journal of the American Statistical Association* **114**(525), 419–433.

- Bura, E., Duarte, S., Forzani, L., Smucler, E. & Sued, M. (2018), ‘Asymptotic Theory for Maximum Likelihood Estimates in Reduced-Rank Multivariate Generalized Linear Models’, *Statistics* **52**(5), 1005–1024.
- Chatelin, F. (1983), *Eigenvalues of Matrices*, New York: Wiley.
- Chen, H., Raskutti, G. & Yuan, M. (2019), ‘Non-Convex Projected Gradient Descent for Generalized Low-Rank Tensor Regression’, *Journal of Machine Learning Research* **20**, 1–37.
- Chen, Y., Luo, Z. & Kong, L. (2021), ‘ $\ell_{2,0}$ -Norm Based Selection and Estimation for Multivariate Generalized Linear Models’, *Journal of Multivariate Analysis* **185**, 104782.
- Donoho, D. L. & Johnstone, I. M. (1994), ‘Minimax Risk over ℓ_p -Balls for ℓ_q -Error’, *Probability Theory and Related Fields* **99**(2), 227–303.
- Fan, J., Gong, W. & Zhu, Z. (2019), ‘Generalized High-Dimensional Trace Regression via Nuclear Norm Regularization’, *Journal of Econometrics* **212**(1), 177–202.
- Gotoh, J., Takeda, A. & Tono, K. (2018), ‘DC Formulations and Algorithms for Sparse Optimization Problems’, *Mathematical Programming* **169**, 141–176.
- Gower, J. C. & Dijksterhuis, G. B. (2004), *Procrustes Problems*, Oxford University Press.
- Han, R., Willett, R. & Zhang, A. (2022), ‘An Optimal Statistical and Computational Framework for Generalized Tensor Estimation’, *The Annals of Statistics* **50**(1), 1–29.
- Hao, B., Zhang, A. & Cheng, G. (2020), ‘Sparse and Low-Rank Tensor Estimation via Cubic Sketchings’, *IEEE Transactions on Information Theory* **66**(9), 5927–5964.
- Hu, J., Lee, C. & Wang, M. (2022), ‘Generalized Tensor Decomposition With Features on Multiple Modes’, *Journal of Computational and Graphical Statistics* **31**(1), 204–218.
- Inglot, T. (2010), ‘Inequalities for Quantiles of the Chi-square Distribution’, *Probability and Mathematical Statistics* **30**(2), 339–351.
- Johnstone, I. & Lu, A. (2009), ‘On Consistency and Sparsity for Principal Components Analysis in High Dimensions’, *Journal of the American Statistical Association* **104**(486), 682–693.
- Kolda, T. & Bader, B. (2009), ‘Tensor Decompositions and Applications’, *SIAM Review* **51**(3), 455–500.
- Kong, D., An, B., Zhang, J. & Zhu, H. (2020), ‘L2RM: Low-Rank Linear Regression Models for High-Dimensional Matrix Responses’, *Journal of the American Statistical Association* **115**(529), 403–424.
- Li, X., Xu, D., Zhou, H. & Li, L. (2018), ‘Tucker Tensor Regression and Neuroimaging Analysis’, *Statistics in Biosciences* **10**, 520–545.
- Luo, Z., Sun, D., Toh, K. C. & Xiu, N. (2019), ‘Solving the OSCAR and SLOPE Models Using a Semismooth Newton-Based Augmented Lagrangian Method’, *Journal of Machine Learning Research* **20**(106), 1–25.

- Nesterov, Y. (2013), ‘Gradient Methods for Minimizing Composite Functions’, *Mathematical Programming* **140**, 125–161.
- Obozinski, G., Wainwright, M. & Jordan, M. (2011), ‘Support Union Recovery in High-Dimensional Multivariate Regression’, *The Annals of Statistics* **39**, 1–47.
- Poythressa, J. C., Ahnb, J. & Parkc, C. (2021), ‘Low-Rank, Orthogonally Decomposable Tensor Regression With Application to Visual Stimulus Decoding of fMRI Data’, *Journal of Computational and Graphical Statistics* **31**(1), 190–203.
- Raskutti, G., Yuan, M. & Chen, H. (2019), ‘Convex Regularization for High-Dimensional Multiresponse Tensor Regression’, *The Annals of Statistics* **47**(3), 1554–1584.
- Rockafellar, R. T. & Wets, R. J. B. (2009), *Variational Analysis*, Vol. 317, Springer Science & Business Media.
- Su, W. & Candès, E. J. (2016), ‘SLOPE is Adaptive to Unknown Sparsity and Asymptotically Minimax’, *The Annals of Statistics* **44**(3), 1038–1068.
- Sun, W. W. & Li, L. (2017), ‘STORE: Sparse Tensor Response Regression and Neuroimaging Analysis’, *Journal of Machine Learning Research* **18**, 1–37.
- Van Essen, D. C., Smith, S. M., Barch, D. M., Behrens, T. E. J., Yacoub, E. & Ugurbil, K. (2013), ‘The WU-Minn Human Connectome Project: An Overview’, *NeuroImage* **80**(15), 62–79.
- Watson, G. A. (1992), ‘Characterization of the Subdifferential of Some Matrix Norms’, *Linear Algebra and its Applications* **170**, 33–45.
- Wei, Q., Zhang, Y. & Zhao, Z. (2021), Sparse Reduced-Rank Regression With Adaptive Selection of Groups of Predictors, in ‘55th Annual Asilomar Conference on Signals, Systems, and Computers’, pp. 145–149.
- Wen, B., Chen, X. & Pong, T. (2018), ‘A Proximal Difference-of-Convex Algorithm With Extrapolation’, *Computational Optimization and Applications* **69**, 297–324.
- Zhang, A., Luo, Y., Raskutti, G. & Yuan, M. (2020), ‘ISLET: Fast and Optimal Low-Rank Tensor Regression via Importance Sketching’, *SIAM Journal on Mathematics of Data Science* **2**(2), 444–479.
- Zhang, T. & Golub, G. H. (2001), ‘Rank-One Approximation to High Order Tensors’, *SIAM Journal on Matrix Analysis and Applications* **23**(2), 534–550.
- Zhou, H., Li, L. & Zhou, H. (2013), ‘Tensor Regression With Applications in Neuroimaging Data Analysis’, *Journal of the American Statistical Association* **108**(502), 540–552.